CANDIDATE THESIS IN CHEMISTRY

HIGH VALENT TRANSITION METAL CORROLE AND CORROLAZINE COMPLEXES:

THE QUESTION OF NONINNOCENT LIGANDS

Espen Tangen

April 2003

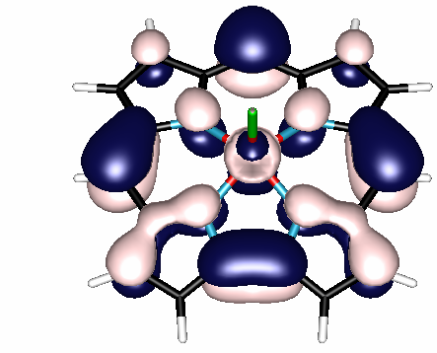

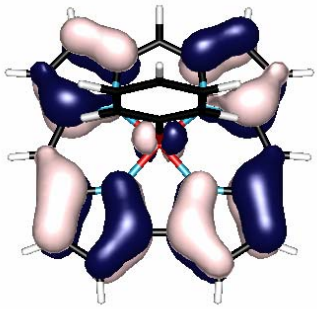

FACULTY OF SCIENCE
Department of Chemistry
University of Tromsø, N-9037 Tromsø

HIGH VALENT TRANSITION METAL CORROLE AND CORROLAZINE COMPLEXES: THE QUESTION OF NONINNOCENT LIGANDS

Espen Tangen

April 2003

Keywords: High valent, iron, manganese, cobalt, corrolazine, corrole, ligand non-innocence, metal-ligand orbital overlap.

Abstract: To contribute to the fundamental picture of the electronic structure of high valent first row transition metal complexes, I have carried out a density functional study of two different macrocyclic ligand systems, corroles and corrolazines, with two different axial ligands, Ph and Cl and a number of different central ions, P(V), Cu(III), Mn(IV) and Fe(IV). DFT calculations on Fe(IV) and Mn(IV) corrole and corrolazine derivatives suggest that compared with the often noninnocent corrole ligands, corrolazines are electronically more innocent and stabilize "purer" high-valent states of transition metal ions. This study also contributes to the idea that (Cor)Fe^{IV}Cl complexes are best regarded as intermediate spin (S=3/2) Fe(III) centers antiferromagnetically coupled to a corrole π-type cation radical, making the corrole ligand noninnocent. The nature of this coupling seems to be an Fe(d_{z^2})-corrole(b_1) orbital interaction for (Cor)Fe^{IV}Cl. For (Cor)Fe^{IV}Ph, however, the situation seems to be different. Like in the Fe(IV) corrole μ-oxo dimers, the corrole ligand has less radical character. DFT(PW91/TZP) studies of (Cor)MPh (M = Fe, Mn, Co) suggests that also metal(d_{zx})-corrole(a_2) orbital interactions may contribute to the ligand noninnocence in high valent metal corrole complexes. In other words, different high-valent metallocorroles may exhibit b_1-type, a_2-type or no radical character.

Front cover: One of high-lying minority-spin MOs of (Cor)MnCl (left) and the majority-spin HOMO of (Cor)CoPh (right).

University of Tromsø
2003

ACKNOWLEDGEMENTS

This work was performed at the Northernmost University in the world, University of Tromsø, where I have been trotting the halls of the Chemistry Department.

I would like to thank my supervisor Prof. Abhik Ghosh for his advice and guidance in the field of science, and for having faith in me despite my frequent delocalization from our laboratory. I would like to thank my coworkers Ingar H. Wasbotten, Erik Steene, Tebikie Wondimagegn, Hege Ryeng, Torgil Vangberg and Renate Lie for guidance during my study.

My calculations were performed mostly on the national supercomputers in Tromsø, and Trondheim, where I was granted computer time by the Research Council of Norway. Having bothered Roy Dragseth, Steinar Trældal-Henden and Tor Johansen a lot, I am grateful for their technical support and also for teaching me things when my computer skills were not sufficient.

The last few months I have been working together with Jeanet Conradie, whose remarks considering my thesis have been valuable, and also Bart van Oort. I want to thank both of you for making our office a nice place to work.

Tromsø, April 2003

Espen Tangen

TABLE OF CONTENTS

1 INTRODUCTION

1.1 INTRODUCTION

Iron is one of the most abundant metals in the earth crust, second only to aluminium. The element is of immense biological importance; the oxygen carriers hemoglobin and myoglobin, the electron transfer proteins cytochromes, and enzymes such as cytochrome P450, soluble methane monooxygenase (sMMO), peroxidases, and nitrogenase all contain iron.[1,2] Both iron(II) and iron(III)-containing molecules occur in biological systems, but Nature also makes use of iron in unusual oxidation states such as +4 in key enzymatic intermediates such as the compound I intermediates of heme proteins and intermediate Q of sMMO.[3]

The macrocyclic porphyrin ligand is widely used in Nature to coordinate iron. Because of the low solubility product of $Fe(OH)_3$, some ligand or other is obviously needed if iron centers are to serve as catalysts in biology and porphyrins, which for in a self-assembly-type process, are well-suited for this. Iron porphyrins, commonly known as hemes, are among the most important of biological cofactors. The question of interest in this thesis is how porphyrin-type ligands, which are relatively easily oxidized, can stabilize strong oxidants such as high-valent iron centers.[3] I have approached this question here using quantum chemical calculations on some high-valent iron porphyrin-type complexes.

At this point, most of the main classes of iron(IV) complexes and intermediates have already been examined by high-quality computational methods in addition to traditional analytical methods. Consequently, a clear picture of the fundamentals of the electronic structure of high-valent iron complexes is beginning to emerge. This work attempts to complete this picture, the specific focus being on iron(IV) corrole and corrolazine complexes and their relevance to heme protein intermediates. As the continuum of this focus, the question of ligand noninnocence in corrole complexes is essential. And not for high valent iron complexes only, but for high valent metal

complexes in general. Thus, this study also includes the neighbouring metals manganese and cobalt.

Before presenting my original results, I will present a brief introduction to crystal field theory, along with relevant examples of transition metal complexes from the metalloporphyrin field.

1.2 AIM OF THIS STUDY

A) Examine the question of ligand-noninnocence in high-valent transition metal corrole and corrolazine complexes.

B) Examine the nature of ligand-metal orbital interactions in transition metal corrole and corrolazine complexes. How do electronic differences in axial ligands influence metal-ligand orbital interactions?

C) These questions led to an analysis of electronic differences between the ring parent systems corroles and corrolazines. How does *meso*-aza-substitution influence high-valent metal ion stabilizing abilities of the ligand?

D) Sketch some possible implications for heme protein intermediates.

For conclusions of this study, the reader is referred to chapter 6.

2 SOME BASIC CONCEPTS

2.1 AN INTRODUCTION TO CRYSTAL FIELD THEORY

Crystal Field Theory (CFT) is a purely electrostatic approach to the bonding within transition metal complexes and was developed to account for spectroscopic properties of *d*-block metal ions in ionic crystals. The basic idea is that a ligand lone pair is modeled as a point negative charge or as the part negative charge of an electric dipole that repels electrons in the *d*-orbitals of the central metal ion. CFT focuses on the resultant energy splitting of *d* orbitals into groups and then uses that splitting to account for number of unpaired electrons in transition metal complexes. Even though this theory ignores covalent bonding interactions between ligands and central metal ions in transition metal complexes, it provides a remarkably good qualitative explanation of many of their properties.

Octahedral coordination complexes

Originally, in CFT, a metal ion was considered surrounded by a uniform sphere of negative charge of some radius *r*. This results in an elevation of all the *d* orbital energies, but they still remain degenerate. If the negative charge is allowed to collect along the coordinate axes in an octahedral arrangement, electrons in the orbitals pointing along the axes (usually d_{z^2} and $d_{x^2-y^2}$) are repelled more than those in the orbitals pointing between the axes (usually d_{xy}, d_{yz} and d_{zx}). The former are raised in energy, the latter are lowered relative to the spherical distribution and the energy of the two doubly degenerate (e_g) orbitals (the d_{z^2} and the $d_{x^2-y^2}$) must be raised 1,5 times as much as the three triply degenerate (t_{2g}) orbitals (the d_{xy}, d_{yz} and d_{zx}) are lowered in order to maintain balance. This is named the Barycentre rule[4,5] and this splitting is named the Ligand Field Splitting (LFS).

The LFS is the simplest property that can be interpreted by CFT. For a complex in an octahedral ligand field, CFT assigns the first absorption maximum in the electronic

spectrum to the transition $e_g \leftarrow t_{2g}$. For complexes with more than one *d*-electron the energy of transition depends on repulsion energies between the *d* electrons also, and the picture gets a bit more complicated.

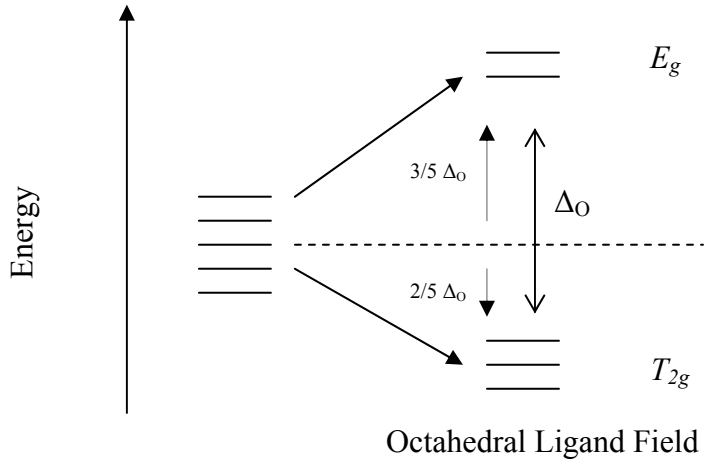

Figure 1: The separation of the orbitals into two sets is called a ligand-field splitting parameter Δ, where a subscript O signifies octahedral complexes.

The ligand field splitting parameter varies systematically with the identity of the ligand, as shown in Figure 1. The spectrochemical series arranges ligands in order of increasing energy of $e_g \rightarrow t_{2g}$ transitions that occur when they are present in a complex, and are presented below for some selected ligands. Ligands generating a weaker ligand field are to the left in the series and ligands generating a stronger ligand field are to the right:[5,6]

$$I^- < Br^- < S^{2-} < Cl^- < NO_3^- < F^- < OH^- < H_2O < NH_3 < En < Bipy < Phen < NO_2^- < CN^- < CO$$

Note that OH^- is a weaker ligand than H_2O, which may seem strange, but this has to do with the fact that the former is better at forming π-bonds which destabilizes the t_{2g} orbitals.

Electronic properties for a complex are intimately related to its central metal ion and it is not generally possible to state whether a particular ligand gives a large or small ligand field splitting parameter without considering the metal ion also. In general Δ increases with increasing oxidation number and increases down a group.

The spectrochemical series for some selected metal ions is approximately:[5]

$$Mn^{2+} < Ni^{2+} < Co^{2+} < Fe^{2+} < V^{2+} < Fe^{3+} < Co^{3+} < Ru^{3+} < Pd^{4+}$$

One possible explanation to this series is that the narrowing of ionic radii from left to right across a period in the periodic system causes the bonding between the ligand and the metal central ion to increase in strength. This series is also thought to reflect the improved metal-ligand bonding of the more expanded *4d* and *5d* orbitals compared with the compact *3d* orbitals. In general *4d* and *5d* metals have larger Δ_O-values than the *3d* metals. Hence, complexes of these metals generally have electron configurations characteristic of strong ligand fields.

Ligand field strength and electron distribution

For an octahedral complex, the first three *d*-electrons of a d^n complex occupy separate t_{2g} orbitals and do so with parallel spins. A d^3 complex is stabilized by $3 * 0{,}4\,\Delta_O = 1{,}2\,\Delta_O$. The next electron needed for the d^4 complex may enter one of the t_{2g} orbitals, pair with an electron already there and experience a strong coulombic repulsion (the pairing energy E_p). Alternatively the electron may occupy one of the e_g orbitals and then have to overcome the Δ_O-barrier. In the $(t_{2g})^4$ case the net stabilization energy is $E_{stab} = 1{,}6\Delta_o - E_p$ and in the $(t_{2g})^3(e_g)^1$ case the net stabilization energy is $E_{stab} = 3 * 0{,}4\,\Delta_O - 0{,}6\,\Delta_O = 0{,}6\,\Delta_O$. So, when adding one electron to an octahedral d^3 complex, if $\Delta_O < E_p$ occupation of the upper orbitals is more favorable because the electron repulsion is minimized and if $\Delta_O > E_p$ pairing is more favorable despite electron repulsion. We call the former the **weak field** case and the latter the **strong field** case, addressing the fact that this is influenced by the ligand field strength. The contribution to this stabilization from the ligand field is called the Ligand field stabilization energy (LFSE).

When there is no competition between the ligand field splitting parameter Δ and the pairing energy E_p, the ground state electron configuration is unambiguous. When alternative configurations are possible, the configuration with the smaller number of

parallel electron spins is called the low-spin configuration and the configuration with the greater number is called the high-spin configuration. If there are more than two options for the given complex, we also may speak about one or more intermediate-spin configurations.

Because the Δ-value depends on both of the metal and the ligands, and the spin pairing energy varies with the metal, it is not possible to specify exactly where the spectrochemical series complexes will changes from high to low spin. In general, *3d* metal complexes with ligands to the right in the spectrochemical series are low spin and *3d* metal complexes with ligands to the left in the spectrochemical series are high spin.

Tetragonal and square-planar coordinated complexes

Typically, copper(II) d^9 and low spin d^7 complexes depart considerably from the octahedral symmetry[5] and have lower energies than pure octahedral ligand field stabilization predicts. The distortion present in these complexes, called a tetragonal distortion, corresponds to an extension or compression along the z-axis and a simultaneous compression or expansion along the x- and y-axes. If one or three electrons occupy the e_g orbitals (as in low-spin-d^7 and d^9 complexes) a tetragonal distortion may be energetically advantageous. In an octahedral d^9 complex, the odd electron can occupy either the $d_{x^2-y^2}$ or the d_{z^2} orbital. A tetragonal distortion can lower the energy of the latter and thereby also the energy of the complex. This is why octahedral copper(II) complexes are rare and copper(II) sites in enzymes are never hexacoordinate. The tetragonal distortion just described is an example of the Jahn-Teller effect: If the ground electronic configuration of a nonlinear molecule is degenerate, then the molecule will distort so as to remove the degeneracy and achieve a lower energy.

Tetragonal distortion of octahedral d^8 ($t_2^6 e_g^2$) complexes may be large enough to encourage the two e_g-electrons to pair in the d_{z^2} orbital, loosening the ligands on the z-axis to give d^8 square planar complexes. One might say that the square planar

geometry is derived from octahedral geometry by removing electronic charge along the z-axis to infinity.

The preponderance of square planar conformation for the $4d^8$ and $5d^8$ metal complexes correlates with large ligand field splitting, which gives rise to a high ligand field stabilization of low spin square planar complexes. $3d^8$ metal complexes typically experience smaller ligand field splitting, so $[NiX_4]^{2-}$ complexes with X a halogen are generally tetrahedral. Only when coordinated by ligand high in the spectrochemical series, $3d^8$ metal complexes will also experience a ligand field splitting large enough to favour the formation of a square planar geometry as for example Ni(II) porphyrin or $[Ni(CN)_4]^{2-}$.

Tetrahedral coordination complexes

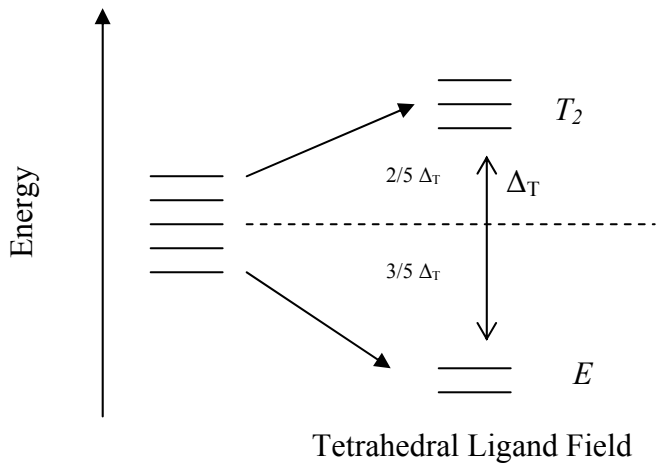

Figure 2: The separation of the d orbitals into two sets in a Tetrahedral Ligand Field. Note that the triply degenerated orbitals are higher in energy than the doubly degenerated orbitals.

The tetrahedral geometry can be considered as derived from a cube, with the metal atom in the center and the ligands pointing toward four particular corners of the cube. This time the negative charges lie between the coordinate axes, and electrons in the d_{xy}, d_{yz} and d_{zx} orbitals are repelled more than those in the d_{z^2} and $d_{x^2-y^2}$ orbitals. None of the orbitals points directly at the negative charge and the separation of the two sets

of orbitals are smaller than in an octahedral ligand field. The Δ_T being less than Δ_O, is also to be expected due to fewer ligands which logically exerts a weaker ligand field.

A tetrahedral crystal field split the *d*-orbitals into two sets, one doubly degenerate and the other triply degenerate, but this time the triply degenerate set lies higher in energy than the doubly degenerate one as shown in Figure 2. This difference from the octahedral *d* orbital splitting can be understood from a detailed analysis of the spatial arrangement of the *d* orbitals, the *e* set being further away from the negative point charge than the t_2 set. Essentially all tetrahedral complexes are high-spin. Figure 3 depicts the ligand field splitting diagrams for a variety of coordination geometries.

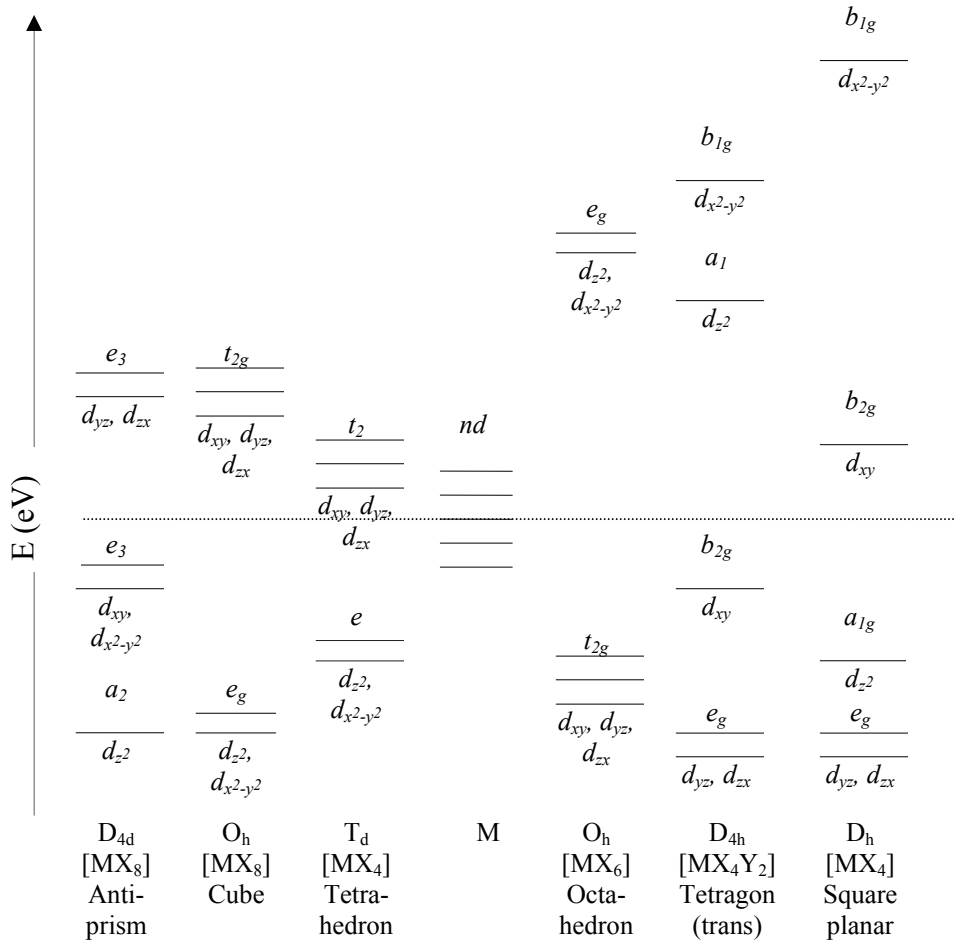

Figure 3. Splitting of d-orbital energy levels in ligand fields of different symmetries. In MX_4Y_2 complexes the splitting of the T_{2g} and the E_g terms can be inverted depending on field strength ration of X/Y.[4, 5, 6]

Molecular Orbital Theory/ Ligand Field Theory

CFT provides a simple model, and as previously mentioned, it does provide a remarkably good and partly quantitative, explanation of a lot of the properties of transition metal complexes. But it has some conceptual weaknesses. For instance the ligand-to-metal charge transfer is hard to explain by only regarding the ligands as negative point charges. Ligand Field Theory (LFT), an application of Molecular Orbital (MO) theory, overcomes this objection. In LFT metal-ligand interactions are considered, with possible orbital overlaps. The key idea is that orbitals with the same symmetry can overlap. So, if the ligand and the metal connect through an σ bonding, there is an orbital overlap between ligand σ orbitals and metal ion orbitals with the same symmetry. The ligand σ orbital has to have σ symmetry around the metal-ligand (M-L) axis.

Likewise, if the ligand and the metal connect through a π bonding, there is an orbital overlap between ligand π orbitals and metal *d* orbitals with π symmetry. A π donor ligand is a ligand that has filled orbitals with π symmetry around the M-L axis. The energies of these orbitals are similar to those of the metal *d* orbitals and the ligand has no low energy vacant π orbitals. A π acceptor ligand has usually empty π orbitals typically lower in energy than metal *d* orbitals available for occupation. Typically the π acceptor orbitals are vacant antibonding orbitals on the ligand.

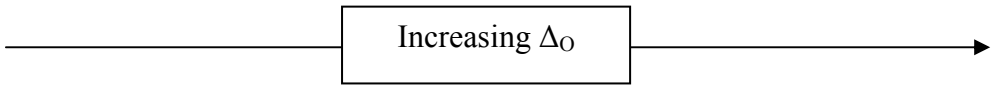

π donor < weak π donor < no π effect < π acceptor

Figure 4: Schematic showing how π-donating abilities of the ligands affects the ligand field splitting parameter.

2.2 PORPHYRINS AND RELATED LIGANDS

Porphyrins

Porphyrins are a large class of deeply colored compounds that play an important role in biology. They owe their bright colors to intense absorptions in the near ultraviolet and visible regions. Porphyrins have been described as "the colour of life"[7] both due to their color and their importance in biology. The word porphyrin is actually derived from the Greek word for purple, porphura.

The best-known natural porphyrin is probably the heme cofactor (iron porphyrin), which is responsible for O_2-transport and storage (as hemoglobin and myoglobin), electron transport (as cytochromes b and c), O_2 activation and utilisation (cytochrome P_{450} and cytochrome oxidase) and sensing (as the NO-sensor soluble guanylate cyclase, the O_2 sensor FixL and the CO sensor CooA).[7] This listing illustrates the biological importance of porphyrins; the main function of porphyrins and porphyrin like ligands is to bind metal atoms that act as centers for significant biochemical events.[7]

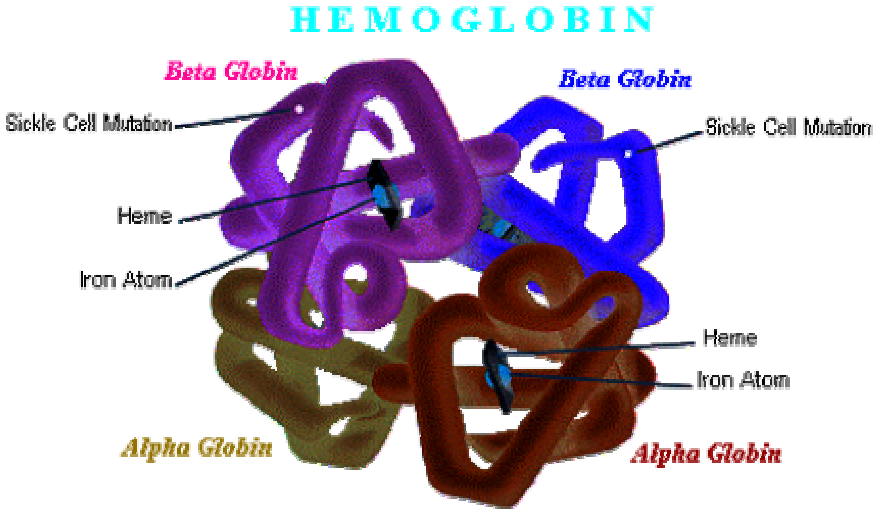

Figure 5: The hemoglobin molecule.[8] Note the heme groups with their iron centers.

The porphyrin skeleton is made by four pyrrole units linked together by four methine bridges. This 22 π-electron system has a [18]annulene substructure, and like typical

aromatic compounds unsubstituted porphyrins are planar. Examples of porphyrin structures are showed in Figure 6.

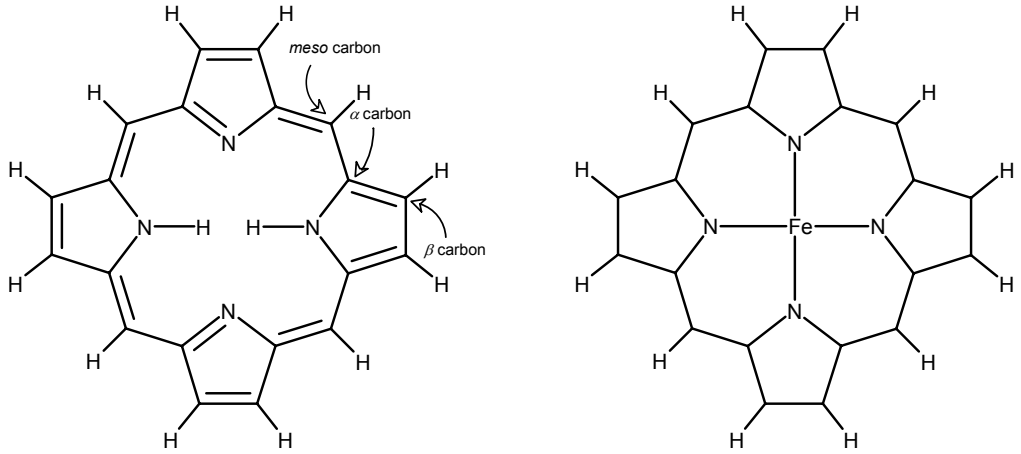

Figure 6: Structure of free base porphyrin (left) and structure of an unsubstituted iron porphyrin (right). Positions of the C_α, C_β and C_m are noted with arrows.

The first simple explanation of the main features of the optical spectra of porphyrins was provided by Goutermans four orbital model.[9,10] According to this model, the two highest occupied molecular orbitals (HOMOs) and two of the lowest unoccupied molecular orbitals (LUMOs) of a typical metalloporhyrin are near degenerate. Furthermore, these four molecular orbitals (MOs) are well separated energetically from the other MOs. Goutermans four-orbital model still is considered a cornerstone in modern porphyrin chemistry, and is highly supported by modern theoretical calculations.[11]

The four-orbital model may be used to predict the energy of the two HOMOs relative to each other. Figure 7 sketches the four frontier orbitals of a metalloporphyrin according to the four orbital model. Due to different amplitudes at the meso positions, it is clear that electron donating or electron withdrawing peripheral substituents affects the a_{1u} and the a_{2u} HOMOs differently. With large amplitudes on the *meso* carbons, the a_{2u} HOMO will be stabilized by electron withdrawing *meso* substituents and destabilized electron donating *meso* substituents. The a_{1u} HOMO has no amplitude at the *meso* positions and is not expected to be strongly affected by *meso*

substituents. On the other hand, substituents in β position should primarily affect the a_{1u} HOMO.[12,13]

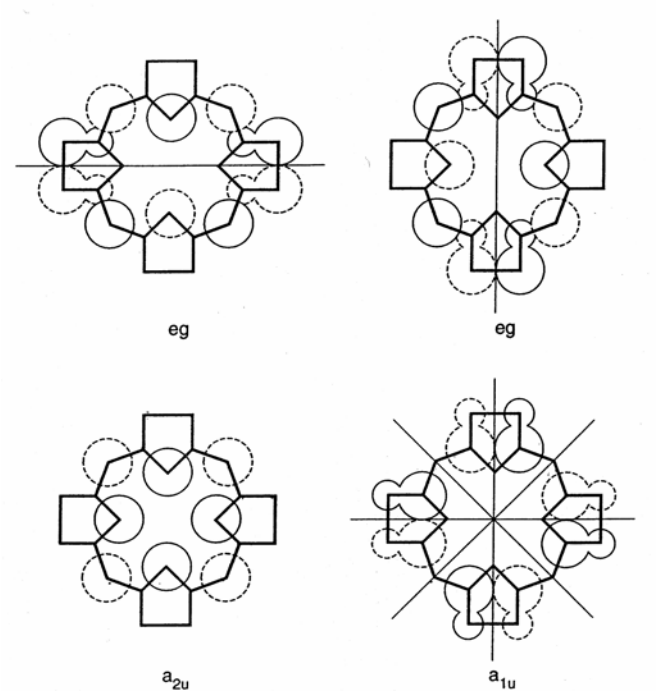

Figure 7: Schematic diagrams of the two porphyrin LUMOs (top) and the two porphyrin HOMOs (bottom) in the four orbital model.[9,10] The representations refer to D_{4h} symmetry.

Free-base porphyrins are amphoteric and suitable bases can abstract the two central protons, the porphyrin dianions thus produced being versatile ligands. Like other aromatic molecules, porphyrins also undergo a number of electrophilic substitution reactions.

Corroles and Corrolazines

Corrole is also based on the [18]annulene structural framework, missing just one *meso* carbon from the porphyrin skeleton, as shown in Figure 6. It is a fully aromatic version of corrin, the tetrapyrrolic ligand of the B_{12} cofactor showed in Figure 8.[2,14]

The missing *meso* carbon leads to a smaller central cavity compared to a porphyrin and reduces symmetry from D_{4h} to C_{2v}. Because of this missing *meso* carbon, free base corrole acts as a trianionic ligand due to three protons in the inner core. Being a

trianionic macrocycle with a comparably small cavity gives corroles excellent chelating properties. The most stable oxidation numbers in metallocorroles are often one positive charge higher than in the case of the analogous metalloporphyrins.[15,16] Their ability to stabilize metal ions in higher oxidation states has resulted in considerable recent interest in the chemistry of metallocorroles.

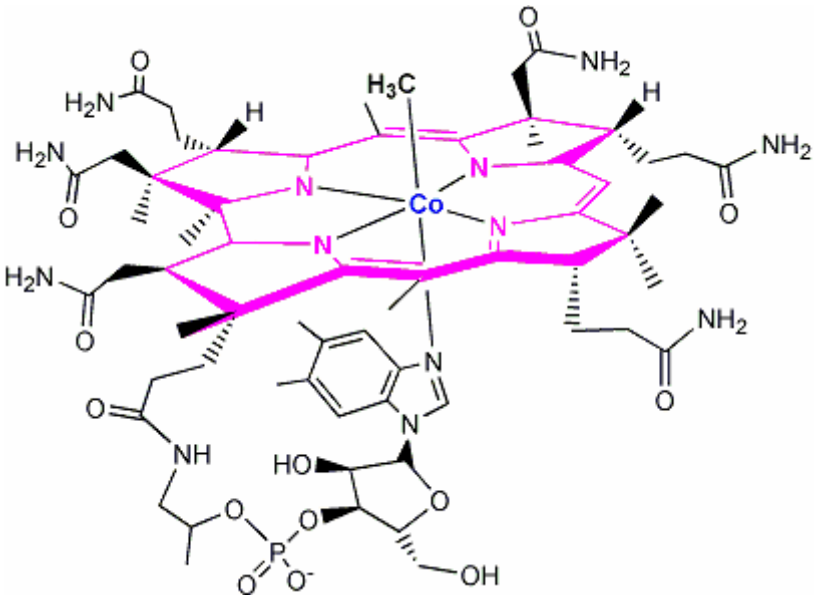

Figure 8: The B_{12} cofactor methylcobalamin.[2,14] The purple color denotes the corrin macrocyle.

Theoretical calculations show that nontransition metal corrole derivatives have two nearly degenerate HOMOs (a_2 and b_1) well separated from the rest of the occupied orbitals and two nearly degenerate LUMOs well separated from the other unoccupied orbitals, as predicted by the Gouterman model.[9,10] As shown in Figure 9, like the porphyrin a_{1u} HOMO the corrole a_2 HOMO has relatively small amplitudes and like the porphyrin a_{2u} HOMO the corrole b_1 HOMO has large amplitudes at the *meso* positions (see also Figure 7).

Bond lengths and bond angles of corrole derivatives show the same order as for corresponding porphyrins: C_α-C_β (1.41-1.44Å) > C_α-C_{meso} (1.39-1.40Å) > C_β-C_β (1.37-1.38Å) ≈ C_α-N (1.37-1.39Å) (see Figure 6 for notation of the carbon atoms).[17] As contracted porphyrins, corroles has a smaller core size than porphyrins. For instance, in (Por)Zn^{II} the adjacent pyrrole nitrogens are separated by 2.87 Å and opposite pyrrole nitrogens are separated by 4.06 Å.

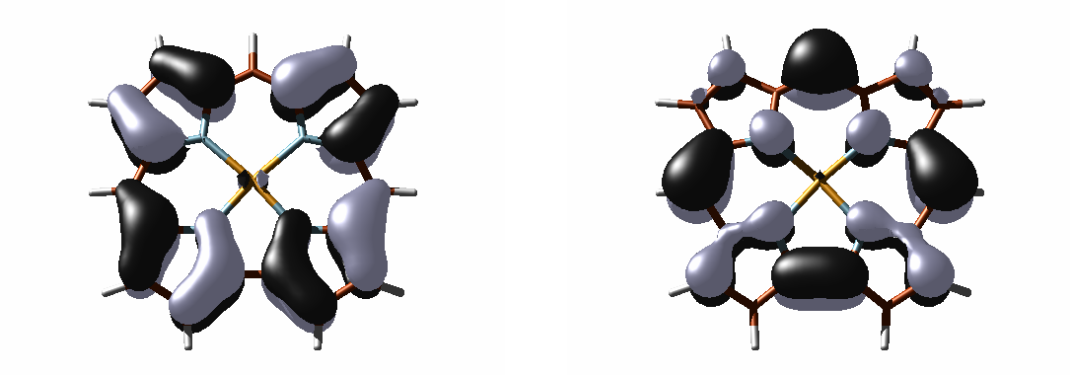

Figure 9: The a_2 (left) and the b_1 (right) HOMOs of (Cor)Cu^{III}, chosen as a representative closed shell metallocorrole.

For a corresponding metallocorrole, (Cor)Ga^{III}, adjacent pyrrole nitrogens are separated by 2.47, 2.71 or 2.83 Å and opposite pyrrole nitrogens are separated by 3.78 Å.[17] Although metal-nitrogen bond length shorter than or equal to 1.90 Å are uncommon for metalloporphyrins, the optimized Ga-N bond distances of 1.89 and 1.91 Å in (Cor)Ga^{III} are typical for metallocorroles.[12,17]

Meso-triazacorroles were first prepared by Ramdhanie et. al[18] and was given the trivial name corrolazine corresponding to porphyrin nomenclature. Corrolazines (Cz^{3-}) differs from corroles by having nitrogens in the *meso* positions as shown in Figure 10, and are related to corroles (Cor^{2-}) by *meso*-azasubstitution, to porphyrazine (Pz^{2-}) by deletion of a *meso* carbon and to porphyrins (P^{2-}) by both.

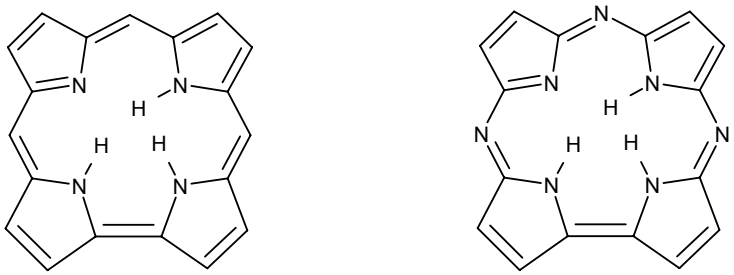

Figure 10: The structure of free base corrole (left) and free base corrolazine (right). Note the three protons in the inner core.

Nonplanar porphyrinoids

Many biological porphyrin cofactors are observed to be nonplanar, and this is suspected to play an important role in biological functions of these compounds.[19,20] Nonplanar distortion may be caused by peripheral steric crowding, electronic interactions involving axial ligands, crystal packing effects, the size of the central ion and specific metal-ligand orbital interactions. For a planar metalloporphyrin with D_{4h} symmetry, the a_{1u} and a_{2u} HOMOs are orthogonal to each of the five metal d orbitals. Specific metal(d)-porphyrin (HOMO) orbital overlaps are switched on by different nonplanar distortions, as listed in Table 1, and these may have important consequences for the chemical and biological properties of metalloporphyrins.

Table 1: Correlation between the standard D_{4h} irreducible representations and the irreducible representations of some relevant lower-order point groups of macrocyclic ligands. For the D_{2d} configuration, there are two possible orientations of the ligand HOMOs.[21] Relevant possible overlaps are marked with colored bold for the given conformation.

Orbitals	Point group					
	D_{4h}	D_{2d}		C_{4v}	C_{2v}	C_s
Metal orbitals	*planar*	*ruffled*	*saddled*	*Domed*		
d_{xy}	b_{2g}	**b_2**	b_1	b_2	a_2	a'
d_{yz}	e_g	e	e	E	b_2	a''
d_{zx}	e_g	e	e	E	b_1	a''
d_{z^2}	a_{1g}	a_1	a_1	**a_1**	a_1	a'
$d_{x^2-y^2}$	b_{1g}	b_1	**b_2**	b_1	a_1	a'
Ligand HOMOs						
a_{1u}	a_{1u}	b_1	b_1	a_2	a_2	a''
a_{2u}	a_{2u}	**b_2**	**b_2**	**a_1**	b_1	a'

For example, ruffling makes the metal(d_{xy})-porphyrin(a_{2u}) orbital interaction symmetry-allowed, where the d_{xy} orbital is the t_{2g}-type d orbital in the porphyrin plane. Saddling turns on the metal($d_{x^2-y^2}$)-porphyrin(a_{2u}) orbital interaction, where the $d_{x^2-y^2}$ orbital is the e_g-type d orbital in the porphyrin plane. Although domed or five-coordinate metalloporphyrins do not necessarily feature significantly nonplanar

porphyrins, I note here that the metal(d_{z^2})-porphyrin(a_{2u}) orbital interaction is symmetry-allowed in such complexes. An analogue of this particular orbital interaction will also be seen to be an important feature of the electronic structures of the high-valent Fe and Mn corroles studied in this work.

2.3 D-ORBITAL SPLITTING DIAGRAMS FOR METALLOPORPHYRINS

Simple crystal field theory is very useful for predicting the *d*-electron configuration of the vast majority of metalloporphyrins. As is standard in CFT, the ligands are assumed to lie along the axes of a Cartesian coordinate system. For a planar porphyrin the x- and y-axes each intersect two pyrrole nitrogens and the z-axis is normal to the porphyrin plane. In an octahedral ligand field, the metal $d_{x^2-y^2}$ orbital is pointing directly towards the pyrrole nitrogens, the metal d_{xy} orbitals is pointing in between the pyrrole nitrogens, the metal d_{yz} and d_{zx} orbitals are pointing between the porphyrin plane and the z-axis, and the metal d_{z^2} orbital is pointing along the z-axis towards axial ligands, if any.

The following figures illustrate examples of *d* orbital splitting diagrams for a few representative metalloporphyrins. The intention has been to establish a correct order of the energy levels for the metal *d* orbitals relevant for the discussion of my results.

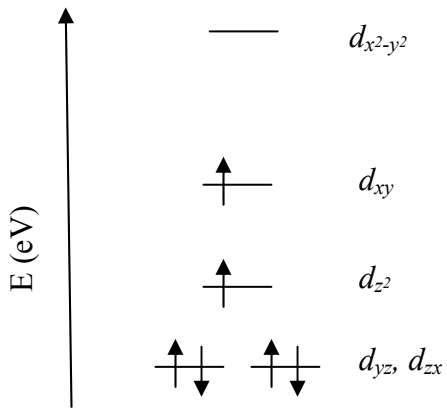

Figure 11: Metal d-orbital splitting for (Por)Fe^{II}, S=1, in a square planar ligand field.[22]

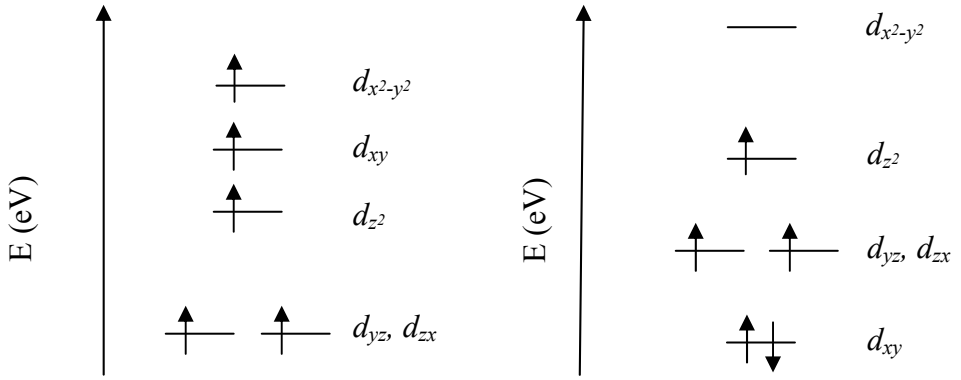

Figure 12: Metal d-orbital splitting for (Por)$Fe^{III}Cl$, S = 5/2 (left) and (Pz)$Fe^{III}Cl$, S = 3/2 (right) in a square pyramidal ligand field. Differences between the two are due to differences in ligand field strength between the field by the porphyrin (Por) ligand and the porphyrazine (Pz) ligand.[23,24]

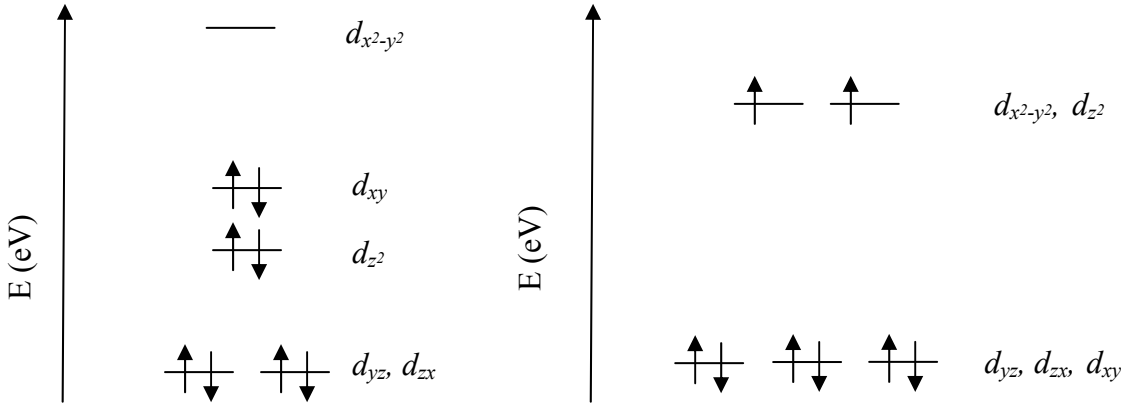

Figure 13: Metal *d*-orbital splitting for (Por)Ni^{II}, S = 0 in a square planar ligand field (left) and (Br_8TPP)$Ni^{II}(Py)_2$, S = 1 in an octahedral ligand field (right).[25,26]

3 HIGH-VALENT TRANSITION METAL PORPHYRINS

3.1 FIRST-ROW TRANSITION METALS

The first row transition metals titanium (Ti), Vanadium (V), Chromium (Cr), Manganese (Mn), Iron (Fe), Cobalt (Co), Nickel (Ni) and Copper (Cu) exhibit more than common oxidation state. Table 2 presents the electron configurations of the different oxidation states for metal complexes (i.e. not bare ions). These metal ions also display a wide range of coordination numbers and geometries.[1]

Table 2: Electronic configuration of the first transition series in different high valent states. High-valent states are indicated in bold red.

Element	**Sc**	**Ti**	**V**	**Cr**	**Mn**	**Fe**	**Co**	**Ni**	**Cu**	**Zn**
Atomic number	**21**	**22**	**23**	**24**	**25**	**26**	**27**	**28**	**29**	**30**
Atoms	$3d^1 4s^2$	$3d^2 4s^2$	$3d^3 4s^2$	$3d^4 4s^2$	$3d^5 4s^2$	$3d^6 4s^2$	$3d^7 4s^2$	$3d^8 4s^2$	$3d^{10} 4s^1$	$3d^{10} 4s^2$
M^{2+} comp.	d^1	d^2	d^3	d^4	d^5	d^6	d^7	d^8	d^9	d^{10}
M^{3+} comp.	d^0	d^1	d^2	d^3	d^4	d^5	d^6	**d^7**	**d^8**	-
M^{4+} comp.	-	d^0	**d^1**	**d^2**	**d^3**	**d^4**	**d^5**	**d^6**	**d^7**	-
M^{5+} comp.	-	-	**d^0**	**d^1**	**d^2**	**d^3**	**d^4**	-	-	-

The specific focus of this thesis is on high-valent transition metal ions, and I choose to define high-valent metal ions as those that are higher-valent than the common oxidation states. These are indicated in bold red in Table 2. In this chapter, I will provide a brief survey of the electronic structures of the major classes of high-valent first row transition metal porphyrins and related complexes.

Why are high-valent transition metal complexes of interest? Many such species occur as the critical reactive intermediates of a variety of oxidative processes such as C-H activation in both Nature (i.e. as metalloenzymes) and industrial processes. Thus, high-valent transition metal complexes are both of fundamental electronic-structural and practical interest.

3.2 SCANDIUM AND ZINC PORPHYRINS

In contrast to other first row transition metals, Scandium (Sc) and Zinc (Zn) exhibit only one stable oxidation state in monoatomic species, +3 and +2 respectively. Sc(III) is a d^0-ion, which implies that no Sc(IV) state are within chemical reach. Similarly, Zn(II) is a d^{10}-ion and highly stable. That basically means that no +3 or +4 states are practically available. Although a theoretical paper by Ghosh and Jynge[17] has reported some quantum chemical calculations on Sc(III) corroles, it is perhaps fair to say that the Sc and Zn porphyrinoids are not of particular interest from an electronic structure point of view, except as a diamagnetic reference. Zn(II) porphyrins are well-known, but not Zn corroles.

3.3 TITANIUM AND VANADIUM PORPHYRINS

The most stable oxidation state of Titanium is Ti(IV). Titanium(IV)-oxo porphyrins are well-known and Ti(IV) corroles have been reported by Licoccia et. al[27] Vanadium(IV)-oxo porphyrins are well-known and these undergo one-electron oxidation to yield V(IV) porphyrin π-cation radicals rather than V(V) porphyrins, as discussed in the following example.

Schulz et. al[28] reported a porphyrin radical complex, $[(OEP^{\bullet})V^{IV}O(OH_2)]SbCl_6$ (OEP = *β*-octaethylporphyrinato), with all spectroscopic data were reported to be consistent with its formulation as a π cation radical complex. Using x-ray crystallography, the vanadium ion was measured to be displaced 0.46 Å towards the oxo axial ligand above the porphyrin mean plane. This is less than the average 0.52 Å displacement seen in other five coordinated vanadyl complexes with known structure.[28] More

importantly, the 2.063 Å value for the average V-N_{Por} (N_{Por} is the porhyrin pyrrole nitrogen) distance is also significantly smaller than the average 2.102 Å value for neutral (OEP)VO or the 2.075 Å value for all the other known five coordinated V complexes.[28] The V-O_{oxo} bond distance was reported to be 1.578 Å in the $[(OEP^{\bullet})V^{IV}O(OH_2)]SbCl_6$. The V-$N_{Por}$ distance may confirm the significant effect of six-coordination, but some changes must also be regarded due to oxidation of the ligand. Because porphyrins have many and complex bonding molecular orbitals, these changes may be less significant.

The conformation of the porphyrinato core in $[(OEP^{\bullet})VO(OH_2)]SbCl_6$ is a S_4 ruffled type not previously reported for a π cation radical derivative, and the complex shows significant A_{1u} ground state characteristics.[29] Most TPP (TPP = *meso*-tetraphenylporphyrin) radicals, on the other hand, are assigned an A_{2u} ground state.[30] The average values for N-C_α is 1.379, C_{meso}-C_α is 1.387 Å, C_α-C_β is 1.447 Å in $(OEP)V^{IV}O$.[28] Room temperature magnetic susceptibility for $[(TPP^{\bullet})V^{IV}O]^+$ have been interpreted as a ferromagnetic coupling of the radical spin with the vanadyl d_{xy} electron (which is orthogonal to the radical orbital if the molecule has local C_{4v} symmetry).[29]

3.4 CHROMIUM PORPHYRINS

The chief high valent oxidation state for chromium is Cr(VI), only a few Cr(V) and Cr(IV) complexes are known, but the latter are important for porphyrins and corroles.[15]

Meier-Callahan et. al[31] made and analyzed an (octaalkylcorrolato)$Cr^{V}O$ complex. An older work by Murakomi et. al[32,33] reported the first oxidation of a $Cr^{V}O$ corrole complex to be metal centered based on UV-vis changes and disappearance of d^1 EPR signal, which would be consistent with the fact that Cr(VI) is a stable oxidation state for chromium. However, Meier-Callahan et. al[34] have argued differently. Using x-ray crystallography they found the metal-oxo bond to be 1.57 Å, the Cr-N_{Cor} (N_{Cor} is the pyrrole nitrogen in the corrole) bond to be 1.93 and the out-of plane metal distortion to be 0.56 Å in two different conformers of (TpFPC)CrO (TpFPC = *meso*-tris-

pentafluorophenylcorrolato). Using EPR spectroscopy supported by ^{1}H NMR spectroscopy, they found that the oxidation of (TpFPC)CrO was ligand centered. The HOMO-LUMO gap, as measured by the difference between the electrochemical oxidation and reduction potentials, for corroles is typically 2.1-2.2 V. This quantity was found to be 1.13 V for (TpFPC)CrO and 0.96 V for (7,8-TEMC)CrO (7,8-TEMC = 7,8-*β*-tetra-ethyl-methylcorrolato),[34] which rules out the possibility that both oxidation and reduction are corrole-centered. An almost identical oxidation potential reported for (TpFPC)CrO and (TpFPC)SnCl suggests that the oxidation on the Cr(V) complex is corrole-centered. The same holds for (octaalkylcorrolato)CrO in comparison with (OEC)SnCl.[34]

Thus, Meier-Callahan et. al[34] reported that (TpFPC)$Cr^{V}O$ was oxidized to $[(TpFPC^{\bullet})Cr^{V}O]^{+}$ but reduced to $[(TpFPC)Cr^{IV}O]^{-}$. Due to strong π(O) donation a Cr(IV) corrole is expected to have a $(d_{xy})^2$ ground state[35] and consistent with this $[(TpFPC)Cr^{IV}O]^{-}$ was reported to be diamagnetic like $(Por)Cr^{IV}O$.[35] A metal-centered oxidation would have yielded an EPR silent d^0 compound, which appeared not to be the case.[34]

A chromium corrole with an almost flat corrole macrocycle and a nearly coplanar mutual alignment of the two coordinated pyridines (Py), [(TpFPCor)$Cr(Py)_2$], was reported to be a Cr(III) corrole complex.[34] The largest deviation reported from the mean plane of the corrole is 0.14 Å. Even though the Cr(III) ion has a somewhat larger radius than the comparable Fe(III) and Co(III) ions, it is still located almost perfectly in the plane of the corrole.[36,37] This is accompanied by a systematic increase in the Cr-N_{Cor} bond distances compared to the M-N_{Cor} bond distances, M = Fe or Co, in related complexes. Samples of (TpFPCor)$Cr(Py)_2$ is reported to display EPR spectra characteristic of Cr(III) (S=3/2) complexes.[34]

For the Cr(IV)-oxo porphyrin complex (TPP)CrO, x-ray crystallographic data collected by Groves et. al.[35] showed a Cr-oxo bond distance of 1.572 Å, an average Cr-N_{Por} bond distance of 2.032 Å, a out-of-plane metal displacement of 0.469 Å with a distinctly nonplanar porphyrin ring.

Table 3: Selected structural parameters for related (TpFPCor)$M^{III}(Py)_2$ complexes.[34] The structures of the complexes are showed in Figure 14, included numbering of the N atoms.

	(TpFPCor)Cr(Py)$_2$	(TpFPCor)Fe(Py)$_2$	(TpFPCor)Co(Py)$_2$
M-N_{Cor} bond lengths (Å)	1.926-1.952	1.865-1.923	1.873-1.900
M-N_{Py} bond length (Å)	2.109, 2.129	2.028, 2.032	1.994, 1.994
N_{21}-N_{23} bond length (Å)	3.871	3.873	3.766
N_{22}-N_{24} bond length (Å)	3.860	3.770	3.775

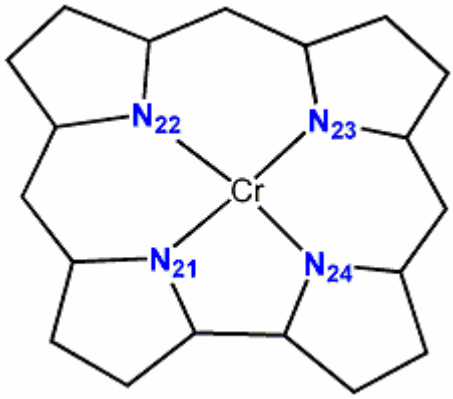

Figure 14: Denotes the numbering of N-atoms referred to in Table 3.

3.5 MANGANESE PORPHYRINS

Manganese exhibits the widest range of oxidation states of any of the first series transition metals. For most parts, however, the inorganic chemistry of manganese is that of the oxidation states II-VII.[1] Further, this section will be concerned with the Mn(III), Mn(IV) and Mn(V) states.

Work by Ghosh, Taylor and coworkers[38] reported theoretical calculations, in agreement with experimental results reported by Kaustov et. al,[39] showing that Mn(IV) and high-spin Mn(III) porphyrin cation radical states are essentially isoenergetic for $[(Por)Mn(PF_6)_2]^0$ (Por = porhyrinato). The same work showed that

$[(Por)MnCl_2]^0$ had a Mn(IV) (S=3/2) state separated from all Mn(III) radical states by at least 1 eV. This indicates that also Mn=O porphyrins are S=3/2, genuine Mn(IV) species. For $(Por)Mn^{IV}O(Py)$ there are reported an optimized Mn=O distance of 1.709 Å, in good agreement with a reported EXAFS value of 1.69 ± 0.03.[40] Corresponding calculated spin populations were found to be 2.25 and 0.71 for the metal and the oxygen, respectively.[38] A *3d* subshell may be spatially contracted in the manganese compound compared to the iron compound, and this is suggested to be responsible for the relative weakness of the Mn(IV)=O bond compared to a Fe(IV)=O bond.[3]

For Mn-oxo porphyrins in formal Mn(V) oxidation states, an important question is whether the ground state corresponds to a Mn(V) species or a Mn(IV) porphyrin cation radical. Both species have been proposed as reactive intermediates[41] but only diamagnetic Mn(V)-oxo porphyrins and corroles are well known.[42,43] For $[(Por)MnO(Py)]^+$, Ghosh et. al.[44] reported a Mn(V) (S=0) ground state with the Mn(IV) porphyrin radical state at least 0.5 eV higher in energy at the DFT (PW91/TZP) level of theory, suggesting that Mn(IV)-oxo porphyrin cation radicals do not exist as ground state species. The optimized Mn=O bond distance of 1.561 Å reported for $[(Por)MnO(Py)]^+$ is in good agreement with experimental distances of 1.548-1558 for Mn(V)-oxo complexes reported by Collins[45,46] and MacDonnell et. al.[47] In contrast to the highly reactive Mn(V)-oxo intermediates, Mn(V)-nitrido complexes are stable and have been known for a long time. The DFT (PW91/TZP) optimized $Mn\text{-}N_{nitrido}$ bond distance for $(Por)Mn^{V}N$ is 1.514 Å.[3]

3.6 IRON PORPHYRINS

Most of the chemistry of iron is that of Fe(II) and Fe(III), but iron in higher oxidation states are also known in a small number of compounds. High valent iron complexes have been detected or proposed as reactive intermediates for various iron enzymes and a number of synthetic models of these enzymes have been proposed also. These models have been studied in detail and a key point of interest in these studies is whether these species are oxidized in a metal- or ligand-centered fashion.

Peroxidase compound I intermediates are formally Fe(V) compounds, but the iron center itself generally cannot sustain a +5 oxidation state. Hence, these intermediates are usually described as Fe(IV)-oxo porphyrin radicals.[48] For both compound I and II intermediates and their models, a common feature appears to be that two unpaired electrons are localized on the ferryl group, distributed approximately 1:1 between iron and oxygen atoms.[49,50] A recent theoretical finding[51] is that the radical in Compound I may not be exclusively localized on the porphyrin, but is partially delocalized on the axial ligand for relatively strongly basic anionic axial ligands such as imidazolate and thiolate. The active site structure of peroxidases has a hydrogen bond between the proximal histidine ligand and a conserved aspartate group. This hydrogen bond has been proposed to impart imidazolate character to the histidine ligand.[52]

To model these effects, Deeth[53] and Green[54] separately reported DFT calculations on both $[(Por)Fe(O)(ImH)]^{+}$ and $[(Por)Fe(O)(Im)]^{0}$ (ImH = Imidazole, Im^{-} = Imidazolate). The former compound appeared to be a normal full-fledged porphyrin radical[49,53,54] whereas more than half of the radical spin appeared to be delocalized onto the imidazolate ligand in the latter compound.[53,54] Deeth[53] also showed that porphyrin ruffling can result in a redistribution of the unpaired electron density of $[(Por)Fe(O)(ImH)]^{+}$, while Vangberg and Ghosh[21] subsequently showed that this redistribution probably results from a metal(d_{xy})-porphyrin(a_{2u}) orbital interaction that becomes symmetry allowed in a ruffled porphyrin (both orbitals transform as b_2 in a D_{2d} ruffled porphyrin as shown in Table 1).

The radical character of the axial thiolate ligand in chloroperoxidase compound I (CPO-I) has been supported by a variety of DFT calculations,[55,56,57] although a resonance Raman study by Hosten et. al.[58] favors an a_{1u} type radical formulation for CPO-I. With respect to the nature and strength of the spin coupling between the radical and the S=1 ferryl group, the different calculations diverge, and both doublet and quartet states have been obtained as ground states for CPO-I models. CPO-I is unique among Compound I intermediates in having an experimentally detected doublet ground state,[59,60] unlike other compound I species which are quartet.[3] For the model complex $[(Por)FeO(SMe)]^{0}$ (SMe = methylthiolate) DFT (B3LYP) calculations

by Green[57] do reproduce this observation, ascribing the doublet state to an antiferromagnetic coupling involving a Fe(d_π)-S(p_π) orbital overlap.

A Fe(V)-oxo perferryl porphyrin intermediate was reported by Murakami et. al,[61] who reported that it most likely can be described as a $[(Por)Fe^{V}O(OMe)]^{0}$ (OMe = methoxide) complex. DFT (PW91/TZP) calculations indicated that much of the radical spin of $[(Por)FeO(OMe)]^{0}$ (S=3/2) was localized on the methoxy oxygen, and thus the iron center cannot be regarded as true Fe(V).[3] The optimized Fe=O bond distance was found to be 1.68 Å, nearly identical to a distance of 1.69 Å in the optimized geometry of the Compound II analogue $[(Por)FeO(OMe)]^{-}$ (S=1), indicating that the electronic character of the ferryl group may be similar in the two compounds.

Results from DFT (PW91/TZP) calculations on peroxidase Compound II model compounds $(Por)Fe^{IV}O$ (C_{4v}, S=1) and $(Por)Fe^{IV}NH$ (C_{4v}, S=1) reported by Dey and Ghosh[62] yielded optimized Fe-O and Fe-N_{imido} distances of 1.634 Å and 1.698 Å, respectively. The optimized Fe-N_{Por} bond distances were reported to be 2.009 Å, the C_α-C_{meso} bond distance 1.387 Å and the C_α-C_{meso}-C_α bond angel 125.6° for the $(Por)Fe^{IV}O$ complex. In both compounds the unpaired electron spins are completely localized on the central Fe-oxo/imido units, the individual spin populations being 1.1985 for the Fe in $(Por)Fe^{IV}O$ and 0.7754 $(Por)Fe^{IV}NH$, 0.8259 for the O in $(Por)Fe^{IV}O$ and 1.2894 for the N_{imido} in $(Por)Fe^{IV}NH$.[62] In $(Por)Fe^{IV}O(Py)$, where the additional pyridine is an axial ligand, the optimized Fe-O distance is reported to be 1.652 Å and the corresponding M-N_{Py} bond length 2.250 Å. There is an expansion of the Fe-O bond length relative to the $(Por)Fe^{IV}O$ complex. As in $(Por)Fe^{IV}O$, the unpaired electron density is completely localized on the ferryl group with the Fe and O spin populations being 1.136 and 0.911 respectively.[3]

The perhaps only examples of true Fe(V) porphyrins, complexes where the *d*-electron occupancy can be described as $(d_{xy})^1(d_{zx})^1(d_{yz})^1$, are the Fe(V) nitrido porphyrin complexes $(OEP)Fe^{V}N$ first isolated by Wagner and Nakamoto.[63,64] Resonance Raman spectral investigations revealed a band that was assigned to a Fe(V)$N_{nitrido}$ stretch on the basis of isotope substitution experiments. To further investigate these

complexes, Dey and Ghosh[62] have carried out some DFT (PW91/TZP) calculations giving an optimized Fe-$N_{nitrido}$ bond distance of 1.722 Å, which is significantly longer than the optimized Fe-O bond distance in (Por)$Fe^{IV}O$ mentioned earlier. For (OEP)$Fe^{V}N$, the optimized Fe-N_{Por} bond distances were reported to be 2.008 Å, the C_{α}-C_{meso} bond distance were reported to be 1.378 Å and the C_{α}- C_{meso} - C_{α} bond angel were reported to be 125.6°.[62]

This may be interpreted in the following manner: Although the Fe-$N_{nitrido}$ stretching frequency of (OEP)$Fe^{V}N$ is higher than the Fe-O stretching frequency of (OEP)$Fe^{IV}O$,[65] the former vibration corresponds to a lower force constant. Dey and Ghosh[62] found the three unpaired electron spins of (Por)$Fe^{V}N$ to be entirely localized on the Fe-$N_{nitrido}$ unit and the Fe and the $N_{nitrido}$ spin populations were 1.579 and 1.550, respectively.

3.7 COBALT PORPHYRINS

The decrease in the stability of high oxidation states from Mn to Fe is continued for Co. Stable simple cobalt compounds are mostly those of Co(II), and low spin octahedral Co(III) complexes are noteworthy for their kinetic inertness.[1] The great interest for organocobalt complexes is influenced by the presence of a cobalt-carbon bond in coenzyme B_{12} (Figure 8) and during recent years, many aryl σ-bonded organocobalt complexes have been synthesized and chemically characterized.

Corrole complexes containing cobalt in formal Co(IV) and Co(V) oxidations states were reported Will et. al. in 1996.[66] These corroles were characterized as (OEC)CoPh and $[(OEC)CoPh]^{+}$ (OEC = *β*-octaethylcorrolato) compounds. In (OEC)CoPh, the out-of plane metal displacement was found to be 0.185 Å, the average Co-N_{Cor} bond distance 1.856 Å and the Co-C_{Ph} bond distance 1.937 Å. Both bond distance values are shorter than the reported M-N_{Cor} and M-C_{Ph} bond distances of (OEC)FePh (1.871 and 1.984, respectively). Because of the small metal ion out-of-plane displacement, the corrole ligand of (OEC)CoPh adopts a nearly planar conformation.

The distribution of unpaired electron density in (OEC)CoPh may be described in two different ways: As a Co(IV) corrole, with the unpaired electron localized on the metal center or as a Co(III) corrole π cation radical, with the unpaired electron delocalized over the corrole macrocycle. EPR data for (OEC)CoPh favour the first formulation and suggest that the complex contains a low spin d^5 Co(IV) ion with an almost pure $(d_{xz}, d_{yz})^4(d_{xy})^1$ configuration.[66] In favour of this conclusion, a large spin delocalization throughout the porphyrin macrocycle is observed for Fe(III) porphyrins having $(d_{xz}, d_{yz})^4(d_{xy})^1$ configuration.[67] I have investigated the electronic structure of these complexes, and the results are given in chapter 5.

In case of the $[(OEC)CoPh]ClO_4$ complex, spectroscopic data indicating a paramagnetic ring current present ruled out the possibility of a Co(V) state.[66] It is interesting to compare the structure of the corrole ligand in $[(OEC)CoPh]ClO_4$ with unoxidized or singly oxidized corrole ligands. An analogous π cation radical containing iron, $[(OEC)FePh]ClO_4$,[68] showed a pattern of alternating short and long bonds in the inner 15-membered ring. This is also the case for the macrocyclic ligand of $[(OEC)CoPh]ClO_4$. The bipyrrolic substructure of $[(OEC)CoPh]ClO_4$ indicates a strong tendency for π bond localization because it contains exceptionally long and short C-N bonds. This is according to theory, which predicts that structures with localized π bonds stabilize the singlet state.[69] Thus, the structure of $[(OEC)CoPh]ClO_4$ are in agreement with the idea that the oxidation and following symmetry break-down of the corrole ligand in (OEC)CoPh leads to a formation of a 4n π electron system.

3.8 NICKEL PORPHYRINS

For Ni, the +2 state is the common oxidation state, Ni(III) and Ni(IV) species being quite rare. Oxidized nickel porphyrin complexes can exhibit a number of valence-tautomeric distributions.25 Depending on the axial ligand, the electron distribution of these complexes corresponds to a low spin Ni(III) tetrapyrrole, a Ni(III) tetrapyrrole π-cation radical or a high spin Ni(II) center. A major reason for interest in nickel-porphyrins is the nickel tetrapyrrole cofactor F_{430} shown in Figure 15.[70]

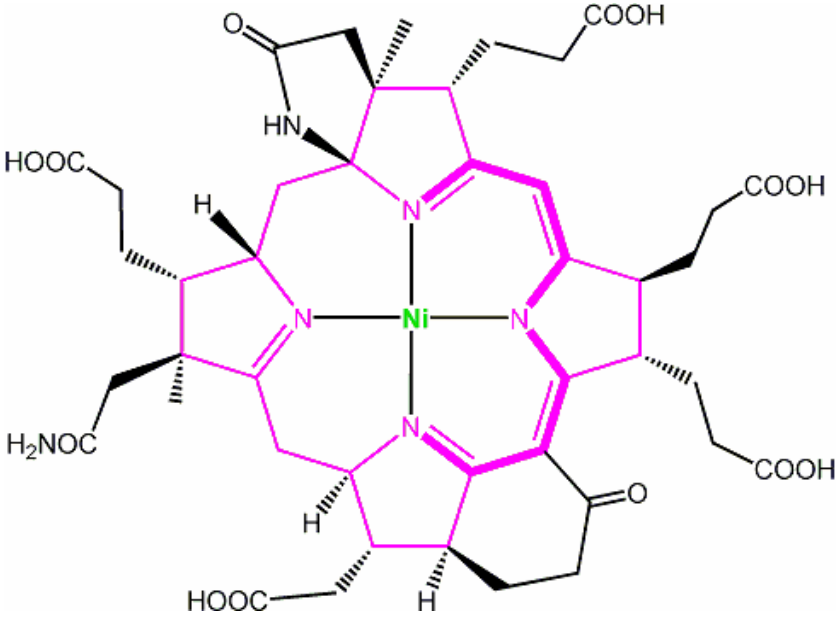

Figure 15: Coenzyme F_{430}70 with its tetrapyrrole skeleton in purple.

Seth et. al.71 have proposed that the unpaired electron in [(TPP)NiIII(Py)2]+ occupies a metal dz2 orbital and in [(TPP)NiIII(CN)2]- occupies a metal dx2-y2 orbital, whereas Fajer25,72 reports a (dz2)1configuration for [(TtBuP)NiIII(CN)2]- (TtBuP = meso-tetra-tert-butylporphyrin). Using DFT (PW91) calculations, Ghosh et. al.73 found that the ground state [(Por)NiIII(Py)2]+ and [(Por)NiIII(CN)2]- corresponds to (t2g)6(dz2)1 and (t2g)6(dx2-y2)1 occupancies, consistent with the findings of Seth et. al.71 For [(Por)NiIII(Py)2]+, the (t2g)6(dx2-y2)1 configuration was calculated to be 0.43 eV above the ground state and for [(Por)NiIII(CN)2]- the (t2g)6(dz2)1 configuration was found to be 0.96 eV above the ground state.73

The explanation for this is that the ligand field generated by the axial pyridine ligands is weaker than the one generated by the equatorial dianionic porphyrin ligand. The cyanide, however, is a powerfully σ-donating ligand, which strongly destabilizes the d_{z^2} orbital relative to the $d_{x^2-y^2}$ orbital. One might say that these results are consistent with classical crystal field theory. In case of $[(Por)Ni^{III}(Py)_2]^+$, the a_{2u} and a_{1u} type Ni(II) porphyrin cation radical states are both higher in energy relative to the Ni(III) $(t_{2g})^6(d_z2)^1$ ground state. Some relevant optimized geometrical parameters of the mentioned Ni(III) porphyrins are as follows: The optimized Ni-N_{Por} bond length for $[Ni^{III}(Por)(Py)_2]^+$ is 1.96 Å and for $[(Por)Ni^{III}(CN)_2]^-$ is 2.06 Å.[73] The relatively long

Ni-N_{Por} bond length in the latter complex may reflect the partial occupancy of the metal $d_{x^2-y^2}$ orbital.

An oxidized nickel porphyrin, $[(OETPP)Ni(BTD)]^+$ (OETPP = *ß*-octaethyl-*meso*-tetraphenylporphyrinato) with an EPR spectrum typical of hexacoordinate Ni(III) and the unpaired electron in the d_{z^2} orbital, is reported by Renner et. al.[72] The Ni-N_{Por} bond distances were found to be 2.00 Å and the Ni-N_{axial} bond distance was found to be 2.23 Å in this complex. These distances are rather long, compared to corresponding bonds in similar complexes characterized by x-ray crystallography.[74] Renner et. al.[72] proposed that the electronic structure of this oxidized nickel porphyrin was best described as a high spin Ni(II) center with a $(t_{2g})^6(d_{z^2})^1(d_{x^2-y^2})^1$ configuration and the $d_{x^2-y^2}$ electron antiferromagnetically coupled to a porphyrin a_{2u} type radical.

This description and the simple $(t_{2g})^6(d_{z^2})^1$ configuration fall on a continuum of possible electron distributions ranging from pure metal-centered oxidation to porphyrin cation radicals and the description by Renner et. al.[72] of the electronic structure appears to be reasonable because the electron-rich OETPP ligand should be prone to form a cation radical.

DFT (PW91/TZP) calculations suggest that for four-coordinate (Cor)Ni, the Ni(II) corrole π-cation radical state are preferred over a Ni(III) state.[75] This is supported by experiments.[76] The UV-vis spectrum of Ni-*β*-octaalkyl corrole exhibits an unusually weak Soret absorption, suggesting a corrole radical. This does reflect the favorable energetics of d^8 square planar complexes, and may be relevant to the general question of how corroles stabilize high valent transition metals.

3.9 COPPER PORPHYRINS

Copper is by a considerable margin the most noble of the first transition series metal. Cu(II) is the most stable state, also Cu(III) and Cu(IV) are known but less stable. Consistent with this, Cu(III) corroles are known and Cu(III) porphyrins are not.[76,77] Results from relevant DFT (PW91/TZP) calculations concerning Cu(III) porphyrinoids are as follows: For (OEP)Cu, the vertical ionization potentials

corresponding to $(d_{x^2-y^2})^1(a_{1u})^1(a_{2u})^2$, $(d_{x^2-y^2})^1(a_{1u})^2(a_{2u})^1$ and $(d_{x^2-y^2})^0(a_{1u})^2(a_{2u})^2$ final cationic states are 6.17, 6.24 and 6.59 eV respectively,[77] consistent with the fact that Cu(III) porphyrins are not known. In contrast, the analogous ionization potential for (OEP)Ag are 6.18, 6.32 and 5.91 eV respectively, consistent with the experimental observation that one-electron oxidation of Ag^{II} porphyrins yields Ag^{III} porphyrin derivatives.[3]

For copper corroles, the relative energies obtained by DFT (PW91/TZP) calculations are 0.00, 0.16 and 0.35 eV of the $(d_{x^2-y^2})^0(a_{1u})^2(a_{2u})^2$ (S=0), $(d_{x^2-y^2})^1(a_2)^1(b_1)^2$ (S=1) and $(d_{x^2-y^2})^1(a_2)^2(b_1)^1$ (S=1) and states, respectively.[75,78] The NMR spectra of a copper octaalkylcorrole exhibit strong temperature dependence; sharp signals were obtained at room temperature, whereas significant line broadening occurred with increasing temperature. This temperature dependent magnetic behavior was ascribed to equilibrium between a diamagnetic d^8 Cu(III) corrole and a paramagnetic Cu(II) corrole π-cation radical of higher energy.[76]

3.10 AN ADDITIONAL NOTE ON EXITED STATES

Steene et. al.[12] and Wasbotten et. al.[77] reported that the Soret-band of the Cu(III), Fe(IV)Cl and Mn(IV)Cl *meso*-triaryl corrole complexes redshifted dramatically with increasing electron-donating character of the *para* substituents on the *meso*-aryl groups. These redshifts is ascribed to significant ligand-to-metal-charge-transfer character in the electron transitions in questions, and appears to be peculiar to high valent tetra pyrroles. The Soret absorption maxima of free-base tetraaryl porphyrins and triaryl corroles, Ni(II) and Cu(II) porphyrins do not exhibit a significant dependence on the electronic character of the *meso*-aryl substituents.[79] Time-dependent DFT (PW91/TZP) calculations on (Cor)Ga and (Cor)Cu reveal a number of ligand-to-metal charge transfer (LMCT) transitions of high oscillator strength in the Soret band region of (Cor)Cu, but not in the case of (Cor)Ga.[80,81] The LMCT transitions in the case of (Cor)Cu involve exitations into LUMO, which is of b_2 symmetry and has predominantly Cu ($d_{x^2-y^2}$) character. The low-energy transitions of (Cor)Ga are all π-π* transitions.[75,77]

4 METHODS

For all the calculations, I have used the ADF program system, the nonlocal gradient corrected Perdew Wang 1991 (PW91) exchange-correlation functional,[82] Slater type triple - ζ plus polarization (TZP) basis sets, a fine mesh for numerical integrations, full geometry optimisations with appropriate symmetry constraints and tight criterias as implemented in the ADF program system.[83] Because the potential energy surface associated with the ligand systems examined may be "soft", the geometry optimizations were carried out with tighter convergence criterias than default of the ADF program package.

Closed- and open-shell molecules were studied with spin-restricted and -unrestricted calculations, respectively, in general. All IPs were calculated as vertical IPs[84] by ΔSCF procedure, as the difference in total energy between the unionized state and the ionized state. [85, 86]

The following molecules were studied: (Cz = corrolazinate, Cor = correlate)

(Cz)$P^{V}Cl_2$	(C_{2v}, S = 0)
(Cz)$P^{V}F_2$	(C_{2v}, S = 0)
(Cz)Cu^{III}	(C_{2v}, S = 0)
(Cz)$Fe^{IV}Cl$	(C_s, S = 1)
(Cz)$Mn^{IV}Cl$	(C_s, S = 3/2).

(Cor)$P^{V}F_2$	(C_{2v}, S = 0)
(Cor)Cu^{III}	(C_{2v}, S = 0)
(Cor)$Fe^{IV}Cl$	(C_s, S = 1)
(Cor)$Mn^{IV}Cl$	(C_s, S = 3/2)
(Cor)CoCl	(C_s, S = 1/2)
(Cor)FePh	(C_s, S = 1) with the axial ligand in two different orientations.
(Cor)MnPh	(C_s, S = 3/2) with the axial ligand in two different orientations.
(Cor)CoPh	(C_s, S = 1/2) with the axial ligand in two different orientations.

A symmetry unique set of Cartesian coordinates is given in the appendix.

5 RESULTS AND DISCUSSION

5.1 A FIRST THEORETICAL STUDY OF CORROLAZINE

A. Corrolazine Vis-a-vis the Gouterman Four-Orbital Model

Figure 16 depicts a quartet of structurally related tetrapyrrolic ligands, porphyrins (PH_2), porphyrazines (PzH_2), corroles ($CorH_3$) and corrolazines (CzH_3). Metalloporphyrazines have consistently higher oxidation potentials than analogous metalloporphyrins.[87,88] *Meso*-azasubstitution is expected to lead to breakdown of the four-orbital model as has been observed for porphyrazine.[12]

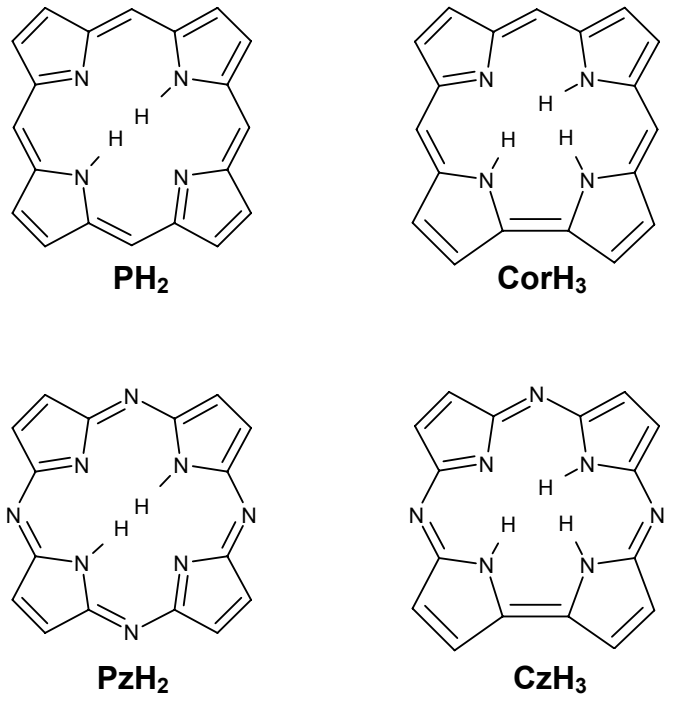

Figure 16: Free-base porphyrin (PH_2), porphyrazine (PzH_2), corrole ($CorH_3$) and corrolazine (CzH_3).

The a_{2u}-type porphyrin HOMO, which has large amplitudes at the *meso* positions, is strongly stabilized by *meso*-aza-substitution. Accordingly, metalloporphyrazines

generally have a_{1u}-type HOMOs and Gouterman's four-orbital model[9,10] does not hold for porphyrazine derivatives.

Also corroles "obey" the Gouterman four-orbital model, the two HOMOs are near degenerate and so are the two LUMOs and these four MOs are energetically well-separated from all other occupied and unoccupied MOs.[75] To check whether the Gouterman four-orbital model holds for corrolazines, I have calculated the two lowest vertical one-electron ionization potentials (IPs) for each of the closed-shell corresponding corrolazine-corrole pair studied. These are as follows, with symmetries of the ionized final states being indicated (comparable values is colored the same way):

(Cor)$P^{V}F_2$:	**($^2A_2$: 7.00 eV, $^2B_1$: 6.82 eV)**	**(Cor)Cu^{III}:**	**($^2A_2$: 6.84 eV, $^2B_1$: 6.73 eV)**
(Cz)$P^{V}F_2$:	**($^2A_2$: 10.28 eV, $^2B_1$: 10.68 eV)**	**(Cz)Cu^{III}:**	**($^2A_2$: 8.18 eV, $^2B_1$: 8.52 eV)**

As we can see, the two lowest IPs are very close to each other for the two corroles, consistent with the four-orbital model, and less so for the corrolazines. These results also indicate higher ionization potentials for corrolazine complexes than for corrole complexes, as expected according to the relationship between porphyrins and porphyrazines, as mentioned above.

Table 4: The DFT(PW91/TZP) orbital energy eigenvalue spectrum of (Cz)Cu^{III}.

Symmetry of orbital	Occupation	Eigenvalue (au)	Energy (eV)
B_1	0.00	-0.11495868128072	-3.128
A_2	0.00	-0.12955218694732	-3.525
B_2	0.00	-0.17174905002396	-4.674
A_2	2.00	-0.19531167692012	-5.315
B_1	2.00	-0.21132146684519	-5.750
A_2	2.00	-0.23528974703818	-6.403
B_1	2.00	-0.2377470704567	-6.469
A_1	2.00	-0.23803710079632	-6.477
A_2	2.00	-0.23981199723731	-6.526

The orbital energy eigenvalue spectrum (Table 4) reveals another interesting feature. The LUMO is not a ligand π MO, but largely derived from the Cu $d_{x^2-y^2}$ orbital. To illustrate this, the various frontier MOs of (Cz) Cu^{III} are shown in Figure 17. This is a feature that the (Cz)Cu^{III} shares with its corrole analogue, (Cor)Cu^{III}.[89]

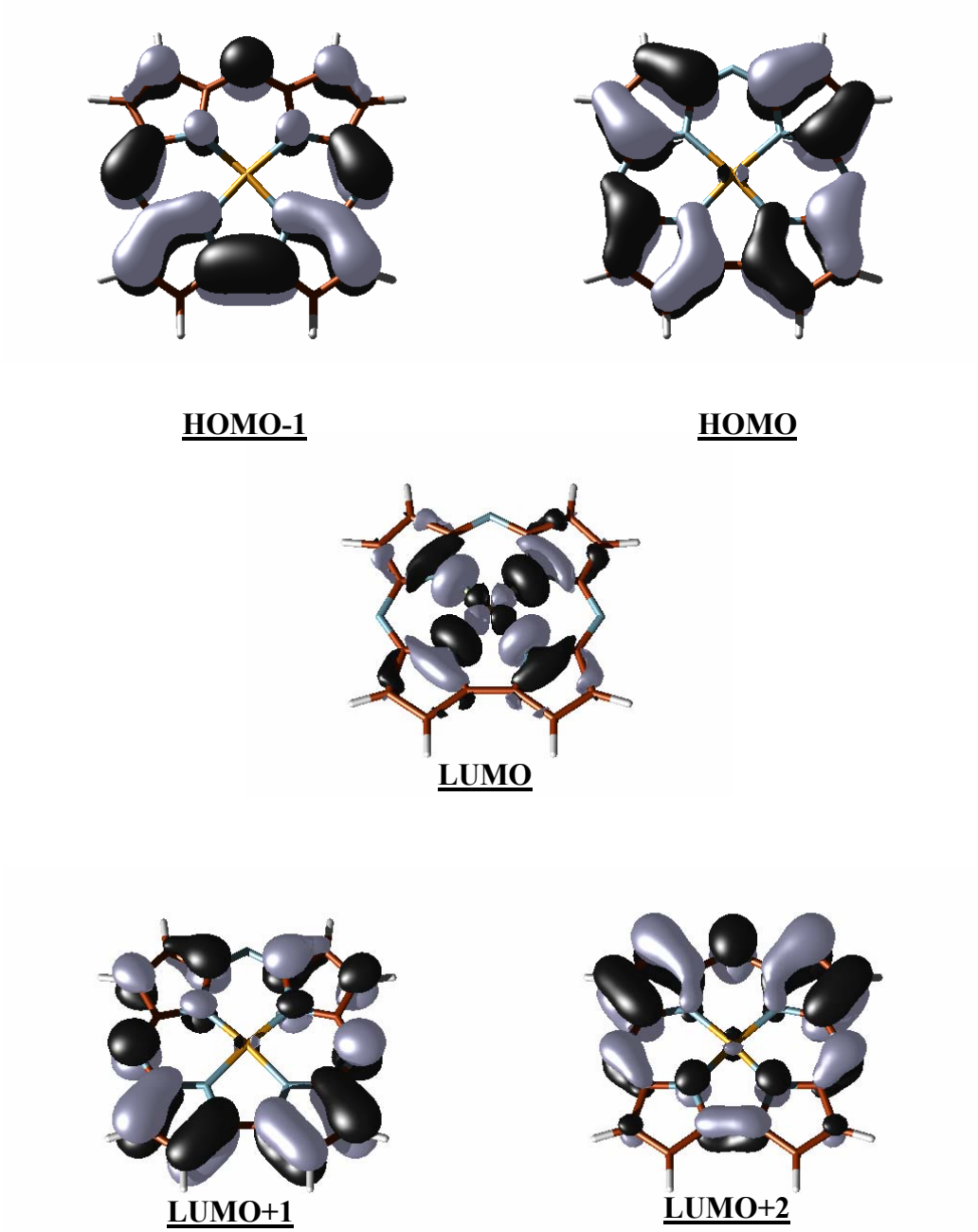

Figure 17: Frontier MOs of (Cz)Cu^{III}. HOMO-1 is the second highest occupied molecular orbital, while LUMO+1 and LUMO+2 is the second lowest unoccupied molecular orbital and the third lowest unoccupied molecular orbital, respectively.

A key question in the aspect of ligand-stabilization of high valent iron, is how corroles do stabilize high-valent transition metal ions with such low oxidation potentials. As shown above, metallocorrolazine may experience a significantly higher oxidation potential compared with a corresponding corrole. This appears to be the case, although an exact parallel with a corrole derivative is not available. Thus, the first oxidation potential of [{(TBP)$_8$Cz}P^V(OH)]OH (TBP = 4-*t*-butylphenyl, Cz = corrolazinato) is rather high, 1.16 V vs. Ag/AgCl (which corresponds to an irreversible oxidation), in spite of the presence of eight electron-donating TBP substituents.[18]

B. Molecular geometries

Figure 18 depicts the DFT(PW91/TZP) optimised geometries of the metallo-corrolazine complexes studied. As expected, the corrolazine core is consistently more contracted than the corresponding corrole core for each central ion considered, Cu(III), Fe(IV), and Mn(IV). Note also the two distinct M-N bond distances in each compound.

The longer M-N distance in each corrolazine complex is about 0.05 - 0.06 Å shorter than the corresponding distance in the analogous corrole complex, as is the case for the shorter M-N distance. This is additionally emphasized in Table 5, which also contains information about the central ion displacement. The Fe(IV) and Mn(IV) ions are displaced about 0.4 Å above the ligand N_4 planes, which is expected for five-coordinate square-pyramidal complexes. These displacements are slightly more for the corrolazine derivatives than for the corrole derivatives, and interestingly, the M-Cl distances in the five-coordinate corrolazine complexes are slightly shorter than those in the analogous corrole complexes.

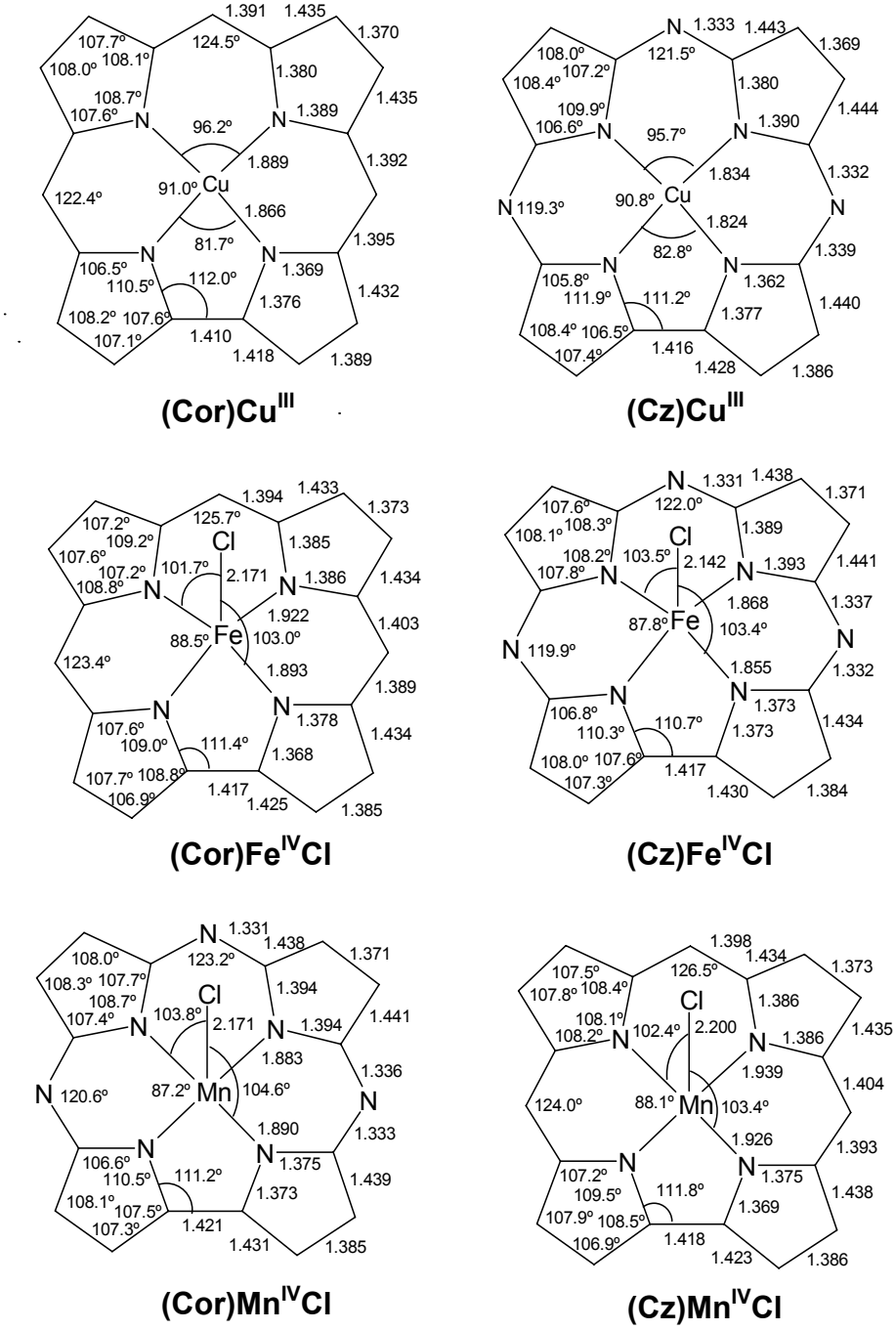

Figure 18: DFT(PW91/TZP) optimised geometries of the metal corrolazines and their corresponding corroles studied.

Table 5: Selected optimised distances (Å), M-N_4 being the displacement of the central atom from the N_4-plane. Numbering of the atoms is illustrated in the figure to the right.

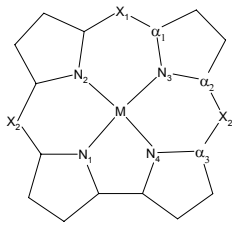

Compound	Corrolazine				Corrole			
M	Cu^{III}	$Fe^{IV}Cl$	$Mn^{IV}Cl$	$P^{V}F_2$	Cu^{III}	$Fe^{IV}Cl$	$Mn^{IV}Cl$	$P^{V}F_2$
M-N_2	1.834Å	1.868Å	1.883Å	1.788Å	1.889Å	1.922Å	1.939Å	1.844Å
M-N_1	1.824Å	1.855Å	1.890Å	1.784Å	1.866Å	1.893Å	1.926Å	1.824Å
$C_{\alpha1}$-X_1	1.333Å	1.331Å	1.331Å	1.326Å	1.391Å	1.394Å	1.398Å	1.384Å
$C_{\alpha2}$- X_2	1.332Å	1.337Å	1.336Å	1.326Å	1.392Å	1.403Å	1.404Å	1.385Å
$C_{\alpha3}$- X_2	1.339Å	1.332Å	1.333Å	1.332Å	1.395Å	1.389Å	1.393Å	1.387Å
M-L_{axial}	-	2.142Å	2.171Å	1.666Å	-	2.171Å	2.200Å	1.656Å
M-N_4	-	0.433Å	0.461Å	-	-	0.407Å	0.431Å	-
N_2-N_4	3.652Å	3.616Å	3.652Å	3.568Å	3.747Å	3.720Å	3.758Å	3.662Å

C. Molecular spin density profiles

Ghosh et. al[16] and Steene et. al.[13] have recently shown that the b_1 corrole HOMO plays a central role in determining electronic character of the corrole ligand in high-valent metallocorrole complexes. With *meso*-triaza-substitution expected to stabilize the corrole b_1 HOMO (shown in Figure 9), a corrolazine radical would be a more unlikely proposition. Thus, ligand innocence is expected for (Cz)FeCl and (Cz)MnCl.

Figure 19 depicts the DFT(PW91/TZP) gross atomic spin populations for the open-shell Fe(IV)Cl and Mn(IV)Cl complexes studied. For both metal ions, there are some systematic differences between the corrolazine versus the corrole derivatives. The metal and Cl spin populations are somewhat lower in the corrolazines than the analogous corroles. However, the main difference between the corrolazine and corrole complexes lies in the spin populations of the *meso* atoms and the central nitrogens. These atoms carry large minority spin populations in the case of (Cor)Fe^{IV}Cl and (Cor)Mn^{IV}Cl, but near-zero or small negative spin populations in the case of (Cz)Fe^{IV}Cl and (Cz)Mn^{IV}Cl. The large negative spin populations in the case of (Cor)Fe^{IV}Cl and (Cor)Mn^{IV}Cl corrole are localized where the macrocycle b_1 HOMO has large amplitudes (see Figure 7 and Figure 9).

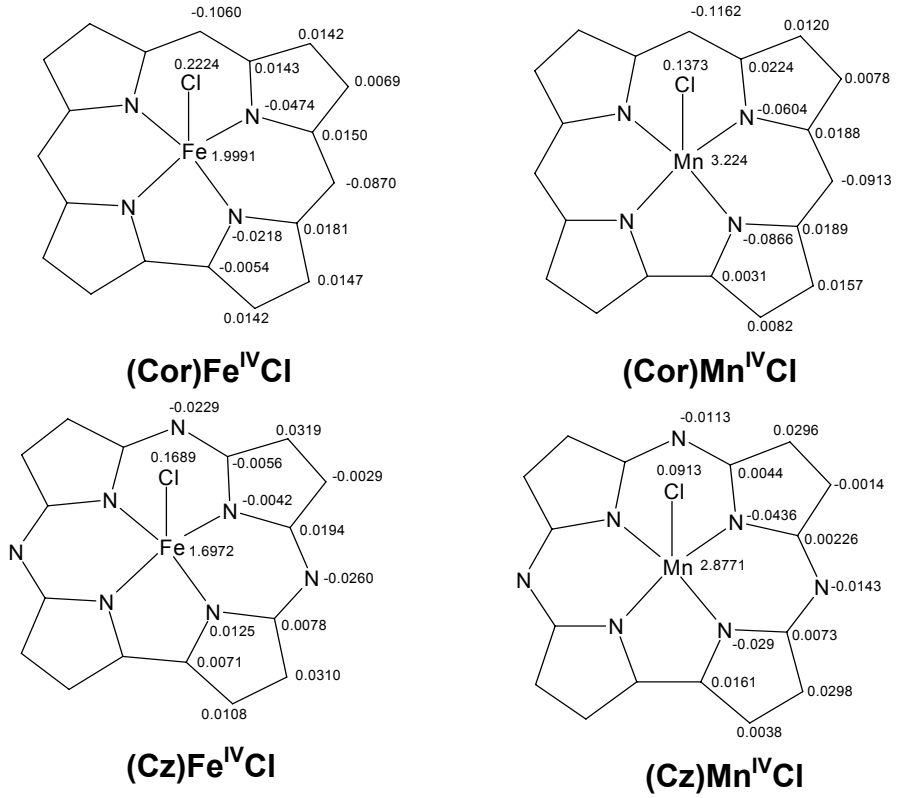

Figure 19: Mulliken gross atomic spin populations from DFT (PW91/TZP) calculations for unsubstituted iron (right) and manganese (left) corrole and corrolazine complexes.

A fair guess would be that for both these molecules, a corrole b_1 radical is antiferromagnetically coupled to an electron in the metal d_{z^2} orbital, which is occupied for Fe(III) (S = 3/2) and Mn(III) (S = 2) centers, as illustrated in Figure 20. The small spin populations - positive or negative - on the corrolazine ligands in (Cz)Fe^{IV}Cl and (Cz)Mn^{IV}Cl complexes indicate a relatively innocent corrolazine ligand and purer high valent Fe(IV) and Mn(IV) centers, compared with (Cor)Fe^{IV}Cl and (Cor)Mn^{IV}Cl.

These results appear to be relevant to a current debate on the nature of high-valent metallocorroles. Based on NMR studies, Cai et. al.[90] proposed a description involving an intermediate spin Fe(III) center antiferromagnetically coupled to a corrole radical for (octamethylcorrolato)Fe^{IV}Cl. Based on electrochemical studies of various formally Fe(IV) and Mn(IV) *meso*-triarylcorrole complexes and on supporting DFT calculations. Ghosh and coworkers[3,75] also reached the same conclusion. In contrast, Simkhovich et. al.[91,92] has favored a clean Fe(IV) description for the

(TpFPC)Fe(IV)Cl complex. My results, however, suggests that both descriptions may be appropriate for different corrole complexes. Like corrolazine, the highly electron-deficient (TpFPC) ligand perhaps does not support a ligand-centered radical, favouring a relatively "pure" Fe(IV) center.

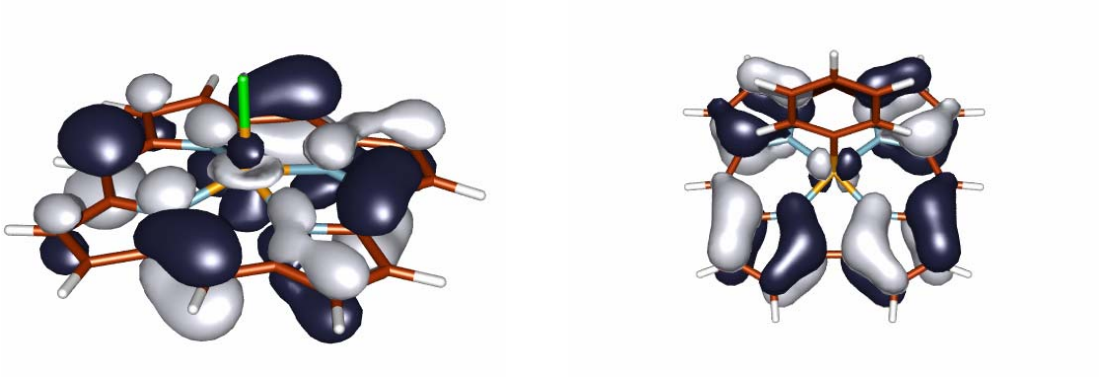

Figure 20: To the left one of high-lying minority-spin MOs of (Cor)MnCl, which illustrates the metal(d_{z^2})-corrole(b_1) orbital interaction. To the right the majority-spin HOMO of (Cor)CoPh, which illustrates a metal(d_π)-corrole(a_2) orbital interaction.

More electron rich metallocorroles, however, like those studied in the labs of Walker[93] and Ghosh,[12] would probably to some greater extent do support a ligand centered radical. Thus, these complexes may feature a (partial) corrole ligand radical. There are, obviously, degrees of ligand noninnocence and any given complex will feature an electronic structure corresponding to a point on the continuum between the two extremes, which are illustrated in Figure 21.

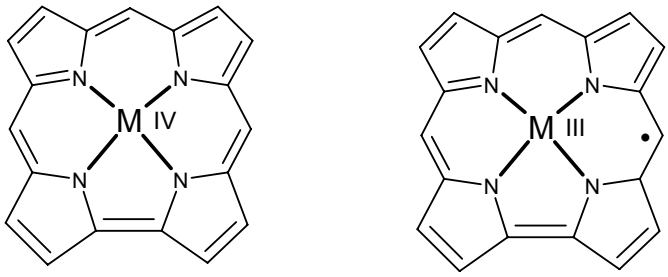

Figure 21: An illustration of the two different electronic structure scenarios, a pure high valent M(IV) metal center coupled to an innocent ligand macrocycle to the left and a reduced M(III) metal center coupled to a noninnocent ligand macrocycle to the right.

Because the N_4 core of corrolazines are extremely contracted, a relevant question to ask is whether the transition metal corrolazine derivatives studied actually can exist as stable compounds. The geometry parameters in the optimized molecular geometries are all reasonable so no particular instability on structural grounds is suspected. Based on the results obtained here, Cu(III), Fe(IV), and Mn(IV) corrolazine derivatives could exist as relatively stable compounds. However, the strongly electron-deficient character of the corrolazine ligand does imply that the Fe(IV) and Mn(IV) complexes may be prone to reduction to the metal(III) oxidation level. The stability of metal corrolazine complexes have later been confirmed by Ramdhanie et. al.[94] and Mandimutsira et. al.[95]

5.2 METAL-LIGAND ORBITAL INTERACTIONS IN METALLOCORROLES

A. Molecular spin density profiles

Previously shown, the corrole a_2 and b_1 HOMOs (Figure 9) crudely resemble the porphyrin a_{1u} and a_{2u} HOMOs (Figure 7). The corrole ligand in many high-valent metal complexes is relatively noninnocent, but Fe(IV)-O-Fe(IV)[12] and Fe(IV)Ph[93] corrole derivatives feature comparatively innocent corrole ligands. As shown in Figure 19, the majority spin density in (Cor)FeCl (S = 1) and (Cor)MnCl (S = 3/2) is almost entirely localized on the metal centers. Significant minority spin density is localized on the pyrrole nitrogens and the *meso* carbons, however, and these positions correspond to significant amplitudes for the corrole b_1 HOMO. The metal(d_{z^2})-corrole(b_1) orbital interaction is depicted in Figure 20 in the form of a minority-spin frontier MO of (Cor)MnCl, which may be responsible for most of the excess minority spin on the corrole ligand in this molecule.

For each (Cor)MPh (M = Fe, Mn, Co) complex, two conformations denoted I and II (Figure 22 and Figure 23) and both with C_s symmetry, were studied. The phenyl ring lies perpendicular to and in the molecular symmetry plane in conformations I and II, respectively. For (Cor)FePh (S =1) and (Cor)MnPh (S = 3/2), the majority spin density (as shown in Figure 22) is largely localized on the metal centers and there is significantly less minority spin on the pyrrole nitrogen and the *meso* carbons

compared to the (Cor)MCl complexes. This may imply less b_1 radical character in the corrole ligand for (Cor)MPh complexes compared to (Cor)MCl complexes (M = Mn, Fe). There is also some majority spin alternating with smaller quantities of minority spin on the phenyl groups. However, a more detailed look reveals somewhat larger minority spin populations on the corrole ring of (Cor)MnPh compared with that of (Cor)FePh, implying a greater degree of b_1 radical character in the former complex.

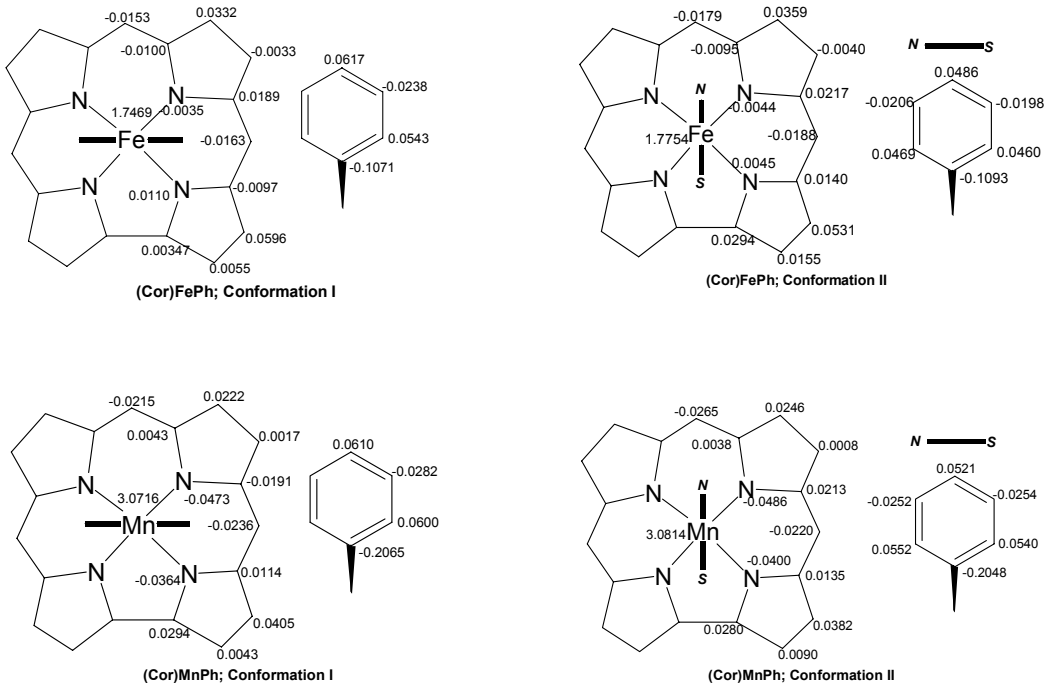

Figure 22: DFT (PW91/TZP) Mulliken spin density profile of (Cor)MPh conformation I (left) and conformation II (right), M = Fe, Mn.

Compared with its Fe and Mn analogues, the spin density profile of (Cor)CoPh (S = 1/2) is quite different, however. The Co center carries less than half the total molecular electronic spin population while certain atoms on the corrole ligand carry relatively large majority electronic spin populations as shown in Figure 23. Thus, only two out of the four nitrogens carry significant majority spin density; again, for any of the four pyrrole rings, only one of the two β carbons (see Figure 6) carries significant majority spin population; finally, the *meso* carbons do not carry any significant spin population. Figure 20, which depicts the HOMO of (Cor)CoPh, illustrates the metal-corrole orbital interaction in the complex. If we examine the spin distribution closely, it appears to match the shape of the corrole a_2 HOMO (Figure 9),

and a fair guess for this complex would be an antiferromagnetically coupling between a corrole a_2 radical and a metal d_π electron.

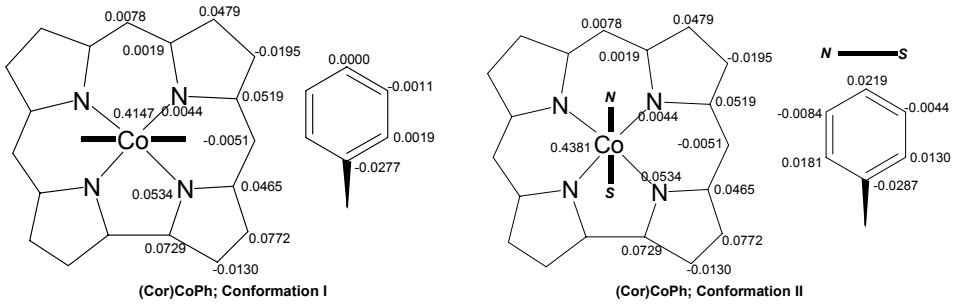

Figure 23: DFT (PW91/TZP) Mulliken spin density profile of (Cor)CoPh conformation I (left) and conformation II (right).

Compared to the Co(III) oxidation state, it seems as if the oxidation equivalent in (Cor)CoPh is distributed roughly evenly between the Co center and the corrole a_2 HOMO. In retrospect, it makes sense that the specific metal d_π AO (d_{zx}) involved in this metal-corrole orbital interaction is the one shown in Figure 20; the other two symmetry-adapted d_π AOs – d_{yz} and d_{xy} - are essentially orthogonal by symmetry to the corrole a_2 HOMO. The metal(d_π)-corrole(a_2) orbital interaction may also be of some importance for (Cor)FePh and (Cor)MnPh. It may account for the small majority spin populations on certain atoms of the corrole ligand.

Zakaharieva et. al.[93] have reported a (Cor)FePh DFT study describing the corrole macrocycle as innocent, which is consistent with findings referred to above, and report of alternating signs of the spin densities on most adjacent atoms, which is reminiscent of that of an "odd-alternant hydrocarbon radical fragment". Specifically, all four nitrogens carry negative spin densities (-0.03 to -0.04), all *meso* carbons also carry negative spin densities (-0.04) and the α carbons have smaller positive spin densities (0.002 - 0.02). This pattern has been previously observed in NMR and EPR studies of such radicals.[90] Based on the above discussion, this "alternant" spin density profile appears to be a superposition of minority-spin B_1-type radical character resulting from a metal(d_{z^2})-corrole(b_1) orbital interaction on the one hand and

majority-spin A_2-type radical character resulting from a metal(d_π)-corrole(a_2) orbital interaction on the other.

Obviously, the metal(d_π)-corrole(a_2) orbital interaction also may exist for (Cor)FeCl and (Cor)MnCl complexes, but largely masked by the metal(d_{z^2})-corrole(b_1) orbital interaction. The latter seems to be the dominant form of metal-ligand orbital interaction, at least for corrole ligand complexes.

B. Structural Chemistry

Table 6 lists various metal-ligand bond distances and metal out-of-plane displacements from the ligand N_4 plane for various optimized metallocorrole structures. These results are also compared with crystallographic results on analogous OEC derivatives.[24,96]

Table 6: Comparison of selected calculated geometry parameters with crystallographic parameters of analogous Mn, Fe, and Co OEC complexes.

Compound	d(M-N_1)	d(M-N_2)	Mean d(M-N)		Δ(M-N_4)		Ref
	Theory	Theory	Theory	Expt.	Theory	Expt.	
MnPh (I)	1.918	1.922	1.920	1.894	0.344	0.286	15
MnPh (II)	1.916	1.925	1.921		0.347		
FePh (I)	1.879	1.903	1.891	1.871	0.316	0.272	96
FePh (II)	1.882	1.930	1.906		0.340		
CoPh (I)	1.858	1.888	1.873	1.856	0.211	0.185	66
CoPh (II)	1.860	1.890	1.875		0.224		
MnCl	1.926	1.939	1.933	1.933	0.431	0.437	15
FeCl	1.893	1.926	1.910	1.906	0.407	0.422	96

The optimized geometries are also in reasonable agreement (±0.02-0.03 Å) with crystallographic geometry parameters on relevant TPP derivatives reported by Goldberg, Gross and coworkers.[36,80,92] For a particular axial ligand, the M-N_{Cor} bonds distance decrease along the period (Mn > Fe > Co), an expected periodic trend. For a particular metal ion, the M-N_{Cor} bond distances are slightly longer in the (Cor)MCl

complexes than in the (Cor)MPh complexes. This may reflect the proposed difference in the metal oxidation state in the two series, +3 in the former versus +4 in the latter. In the (Cor)MPh series, the metal-axial ligand bond distances are slightly longer for Mn than for Fe and Co. All of these trends are according to expectations.

The metal-ligand orbital interactions previously described, may be used to explain some substantial differences in metal out-of-plane displacements observed in the crystal structures of various five-coordinate metallocorroles in the following manner:[24,80,92,97] Metal(d_{z^2})-corrole(b_1) orbital interaction may favor a significant metal out-of-plane displacement because an in-plane metal position would make the metal d_{z^2} and corrole b_1 MOs orthogonal. In contrast, the metal(d_π)-corrole(a_2) orbital interaction would favor an in-plane position of the metal center. Thus, the large (> 0.4 Å) out-of-plane displacements of the metal centers in the (Cor)MnCl and (Cor)FeCl molecules could account for a substantial metal(d_{z^2})-corrole(b_1) orbital interaction. On the other hand, the significantly smaller (~ 0.2 Å) out-of-plane of the Co center in (Cor)CoPh complexes, may enhance the possibility for a significant metal(d_π)-corrole(a_2) orbital interaction as proposed above.

Also as discussed above, the metal(d_{z^2})-corrole(b_1) orbital interaction may be less important for the (Cor)MPh complexes than for the (Cor)MCl (M = Mn, Fe) complexes. The metal(d_π)-corrole(a_2) orbital interaction may be somewhat important in these cases, as reflected in a few significant majority spin populations on the corrole ring (Figure 23). This would account for intermediate metal out-of-plane displacements (~ 0.3 Å) in (Cor)MnPh and (Cor)FePh. For another well known strong electron donating axial ligand, the *μ-oxo* ligand in Fe(IV)-O-Fe(IV) corroles, the metal out-of-plane displacement is about 0.4 Å[80,97] above the N_4 plane. Without explicitly having studied the Fe(IV)-O-Fe(IV) complexes by computational methods, I cannot comment on their detailed structures with any degree of confidence. However, a reasonable guess may be that the metal(d_π)-corrole(a_2) orbital interaction contributes insignificantly to the positioning of the metal center in Fe(IV)-O-Fe(IV) corroles, because the relevant d_π orbitals are coupled in strong Fe(d_π)-O(p_π)-Fe(d_π) three-center π-bonding.

6 CONCLUSIONS

The main conclusions from this study may be summarized in the following:

A) It has been recognized for some time that the corrole ligand in many high-valent metallocorroles is significantly noninnocent, i.e. has radical character. The first oxidation potential of the Fe(IV) corrole chloride complexes are considerably higher than those of the corresponding Fe(IV) corrole μ-oxo dimers, suggesting that the these complexes have distinct differences in their electronic structures. NMR-studies by Cai et. al.,[90] DFT-studies by Ghosh et. al.[12] and comparable DFT calculations on (Cz)$M^{IV}Cl$ and (Cor)$M^{IV}L_{ax}$ (M = Mn, Fe, Co and L_{ax} = Cl, Ph) from this study indicates that (Cor)$Fe^{IV}Cl$ complexes are best regarded as intermediate spin (S=3/2) Fe(III) centers antiferromagnetically coupled to a corrole π-type cation radical, making the corrole ligand noninnocent.

B) DFT(PW91/TZP) calculations have clarified the nature of this antiferromagnetic coupling and attribute it to an Fe(d_{z^2})-corrole(b_1) orbital interaction for (Cor)$Fe^{IV}Cl$. For (Cor)$Fe^{IV}Ph$ and (Cor)$Mn^{IV}Ph$, however, the situation seems to be different. Like in the Fe(IV) corrole μ-oxo dimers, the corrole ligand has less radical character in these complexes. DFT(PW91/TZP) studies of (Cor)MPh (M = Fe, Mn, Co) suggests that also Fe(d_{zx})-corrole(a_2) orbital interactions may contribute to the electronic structure of iron corrole complexes. Thus, it seems as if *both* the corrole a_2 and b_1 HOMOs play an important role in determining the overall electronic spin density profiles of metallocorroles, and they contributes differently to the central ion out-of-plane displacement widely seen in five-coordinated metallocorroles.

C) Reported variations in redox potential among the different Fe(IV) complexes studied indicate that *meso*-aryl substituents can strongly modulate the electronic nature of metallocorrole complexes. This is consistent with the fact

that electron donating and electron withdrawing substituents are expected to destabilize or stabilize, depending on the site of substitution, the corrole a_2 and b_1 HOMO relative to eachother. By substituting carbons in β or *meso* positions with more electron withdrawing atoms (N or F), the ring is expected to be less electron rich and therefore less likely to be partly oxidized (noninnocent). By this substitution one would expect the metal valence to be "purer", in the sense that the real valence of the metal is going to be close to the formal valence. DFT (PW91/TZP) calculations on $(Cz)M^{IV}Cl$ (M=Fe, Mn) from this study confirms this.

D) $(Cor)M^{IV}Cl$ complexes may be regarded as analogues to a five-coordinate $[(Por^{\bullet})FeCl]^{+}$ radical and to HRP-I[98] (Horse Radish Peroxidase compound I), the electronic structure believed to involve a high-spin Fe(III) center anti-ferromagnetically coupled to a porphyrin radical. Similarly, the radical in HRP-I is believed also to be localized mainly on the porphyrin ligand. Regarding compound II intermediates, an interesting possibility is that the ferryl group in CPO-II (Chloroperoxidase compound II) may actually be protonated, i.e. an Fe OH group, instead of CPO-II being a high-valent iron–oxo intermediate. An OH group, like the axial Cl ligand in Fe(IV)Cl corroles, would be less able to stabilize a high-valent iron center than a terminal oxo ligand, as indicated be DFT(PE91/TZP) calculations in this study also.

E) Finally, in terms of future plans, I would like to further contribute to this field in the following two ways:
   i) Through high-level *ab initio* calculations to benchmark the DFT results on corroles.
   ii) Using increasingly efficient DFT codes to study large and complex porphyrinoid systems that are not readily studied by the methods and codes we have used so far.

7 REFERENCES

[1] Sharpe, A. G.; *Inorganic Chemistry*; Longman Scientific & Technical, Harlow, 1992.
[2] Lippard, S. J; Berg, J. M.; *Principles of Bioinorganic Chemistry*; University Science Books, Mill Valley, 1994.
[3] Ghosh, A.; Steene, E. *J. Biol. Inorg. Chem*. **2001**, 6, 739.
[4] Owen, S. M.; Brooker, A..T.; *A Guide to Modern Inorganic Chemistry*; Longman Scientific & Technical, Harlow, 1991.
[5] Schriver, D. F.; Atkins, P. W.; Langford, C. H.; *Inorganic Chemistry 2.ed*; Oxford University Press, Oxford, 1994.
[6] Bersuker, I. B.; *Electron Structure and Properties of Transition Metal Compounds*; John Wiley & Sons, New York, 1996.
[7] Milgrom, L. R.; *The colours of Life*; Oxford University Press, Oxford, 1997.
[8] Graphic obtained from http://www.people.virginia.edu/~rjh9u/hemoglob.html
[9] Gouterman, M. *J. Mol. Spectrosc*. **1961**, 6, 138.
[10] Gouterman, M. *In* D. Dolphin (ed) *The Porphyrins*, Academic Press, New York, **1978**, Vol 3, 1-165.
[11] Ghosh, A.; Vangberg, T. *Theor. Chem. Acc*. **1997**, *97*, 143-149.
[12] Ghosh, A. *In* K. M. Kadish, K. M. Smith, R. Guilard (eds) *The Porphyrin Handbook*, Academic, San Diego, 2000, Vol. 7, Ch 47, pp 1-38.
[13] Steene, E.; Wondimagegn, T.; Ghosh, A. *J. Phys. Chem. B*. **2001**, 105, 11406.
[14] Banerjee, R.; *Chemistry and Biochemistry of B_{12}*; John Wiley & Sons, New York, 1999
[15] Erben, C.; Will, S.; Kadish, K. *In* K. M. Kadish, K. M. Smith, R. Guilard (eds) *The Porphyrin Handbook*, Academic, San Diego, 2000, Vol. 3, Ch 12, pp 233-300.
[16] Ghosh, A.; Steene, E. *J. Inorg. Biochem*. **2002**, 91, 423.
[17] Ghosh, A.; Jynge, K. *Chem. Eur, J.* **1997**, 3, 823.
[18] Ramdhanie, B.; Stern, C. L.; Goldberg, D. P. *J. Am. Chem. Soc*, **2001**, 123, 9447.
[19] Scheidt, W. R.; Lee, Y. J. *Struct. Bond.* **1987**, 64, 1.
[20] Shelnutt, J. A.; Song, X. Z.; Ma, J. G.; Jia, S. L.; Jentzen, W.; Medforth, C. J. *Chem. Soc. Rev.* **1998**, 27, 31.
[21] Vangberg, T.; Ghosh, A. *J. Am. Chem. Soc*. **1999**, 121, 12154.
[22] Grinstaff, M. W.; Hill, M. G.; Birnbaum, E. R.; Schaefer, W. P.; Labinger, J. A.; Gray, H. B. *Inorg. Chem*. **1995**, 34, 4896.
[23] Fitzgerald, J. P.; Haggerty, B. S.; Rheingold, A. L.; May, L.; Brewer, G. A. *Inorg. Chem*., **1992**, *31*, 2006.
[24] Ghosh, A.; Gonzalez, E.; Vangberg, T.; Taylor, P. R. *J. Porphyrins Phthalocyanines* **2001**, *5,* 187.
[25] Renner, M. W.; Fajer, J. *J. Biol. Inorg. Chem.* **2001**, 6, 823.
[26] Duval, H.; Bulach, V.; Fischer, J.; Weiss, R. *Inorg. Chem*. **1999**, 38, 5495.
[27] Licoccia, S.; Paolesse, R.; Tassoni, E.; Polizio, F.; Boschi, T. *J. Chem. Soc. Dalton Trans.* **1995**, 3617.
[28] Schulz, C. E.; Song, H.; Lee, Y. J.; Mondal, J. U.; Mohanrao, K.; Reed, C. A..; Walker, F. A.; Scheidt, W. R. *J. Am. Chem. Soc*. **1994**, 116, 7196.
[29] Erler, B. S.; Scholz, W. F.; Lee, Y. J.; Scheidt, W. R.; Reed, C. A. *J. Am. Chem. Soc.* **1987**, 109, 2644.
[30] Vangberg, T.; Lie, R.; Ghosh, A. *J. Am. Chem. Soc.* **2002**, 124, 8122.
[31] Meier-Callahan, A. E.; Gray, H. B.; Gross, Z. *Inorg. Chem*, **2000**, 39, 3605.
[32] Murakomi, Y.; Matsuda, Y.; Yamada, S. *J. Chem. Soc. Dalton Trans*. **1981**, 855.
[33] Yamaguchi, K.; Watanabe, Y.; Morishima, I. *J. Chem. Soc. Chem. Comm*. **1992**, 1721.
[34] Meier-Callahan, A. E.; Di Bilio, A. J.; Simkhovich, L.; Mahammed, A.; Goldberg, I.; Gray, H. B.; Gross, Z. *Inorg. Chem*. **2001**, 40, 6788.
[35] Groves, J. T.; Kruper, J. W. J.; Haushalter, R. C.; Butler, W. M. *Inorg. Chem.* **1982**, 21, 1363.
[36] Simkhovich, L.; Mahammed, A.; Goldberg, I.; Gross, Z. *Chem. Eur. J*. **2001**, 7, 1041.
[37] Mahammed, A.; Giladi, I.; Goldberg, I.; Gross, Z. *Chem. Eur. J*. **2001**, 7, 4259.
[38] Ghosh, A.; Gonzales, E; Vangberg, T.; Taylor, P. *J. Porhyrins Phthalocyanines*, **2001**, 5, 345.
[39] Kaustov, L.; Tal, M. E.; Shames, A.I.; Gross, Z. *Inorg. Chem*. **1997**, 36, 3503.

[40] Ayougou, K.; Bill, E.; Charnock, J. M.; Garner, C. D.; Mandon, D.; Trautwein, A. X.; Weiss, R.; Winkler, H. *Angew. Chem. Int. Ed. Engl*. **1995**, 34, 343.
[41] Arasasingham, R. D.; Bruice, T. C. *Inorg. Chem*. **1990**, 29, 1422.
[42] Jin, N.; Groves, J. T. *J. Am. Chem. Soc*. **1999**, 121, 2923.
[43] Gross, Z.; Golubkov, G.; Simkhovich, L.; *Angew. Chem. Int. Ed*. **2000**, 39, 4045.
[44] Ghosh, A.; Gonzales, E. *Israel J. Chem*. **2000**, 40, 1.
[45] Collins, T. J.; Gordon-Wylie, S. W. *J. Am. Chem. Soc*. **1989**, 111, 4511.
[46] Collins, T. J.; Powell, R. D.; Slebodnick, C.; Uffelman, E. S. *J. Am. Chem. Soc*. **1990**, 112, 899.
[47] MacDonnell, F. M.; Fackler, N. L. P.; Stern, C.; O´Halloran, T. V. *J. Am. Chem. Soc*. **1994**, 116, 7431.
[48] Terner, J.; Gold, A.; Weiss, R.; Mandon, D.; Trautwein, A. X. *J. Porphyrins Phtalocyanines*, **2001**, 5, 357.
[49] Kuramochi, H.; Noodleman, L.; Case, D. A. *J. Am. Chem. Soc*. **1997**, 119, 11442.
[50] Ghosh, A.; Almlöf, J.; Que, L. Jr. *J. Phys. Chem.* **1994**, 98, 5576
[51] Antony, J.; Grodzicki, M.; Trautwein, A. X. *J. Phys. Chem. A*. **1997**, 101, 2692.
[52] Gajhede, M.; Schuller, D. J.; Henriksen, A.; Smith, A. T.; Poulos, T. *Nat. Struct. Biol*. **1997**, 4, 1032.
[53] Deeth, R. J. *J. Am. Chem. Soc*. **1999**, 121, 6074.
[54] Green, M. T. *J. Am. Chem. Soc*. **2000**, 122, 9495.
[55] Filatov, M.; Harris, N.; Shaik, S. *J. Chem. Soc. Perkins trans*. **1999**, 2, 399.
[56] Harris, D. L.; Loew, G. *J. Am. Chem. Soc*. **1998**, 120, 8941.
[57] Green, M. T. *J. Am. Chem. Soc*. **1999**, 121, 7939.
[58] Hosten, C. M.; Sullivan, A. M.; Palaniappan, V.; Fitzgerald, M. M.; Terner, J. *J. Biol. Chem*. **1994**, 269, 13966.
[59] Rutter, R.; Valentine, M.; Hendrich, M. P.; Hager, L. P.; Debrunner, P. G. *Biochemistry*, **1983**, 22, 4769.
[60] Rutter, R.; Hager, L. P.; Dhonau, H.; Hendrich, M. P.; Valentine, M.; Debrunner, P. G. *Biochemistry*, **1984**, 23, 6809.
[61] Murakami, T.; Yamaguchi, K.; Watanabe, Y.; Morishima, I. *Bull. Chem. Soc. Jpn*. **1998**, 71, 1343.
[62] Dey, A.; Ghosh, A. *J. Am. Chem. Soc*, **2002**, 124, 3206.
[63] Wagner, W. D.; Nakamoto, K. *J. Am. Chem. Soc*. **1988**, 110, 4044.
[64] Wagner, W. D.; Nakamoto, K. *J. Am. Chem. Soc*. **1989**, 111, 1590.
[65] Proniewcz, L. M.; Bajdor, K.; Nakamoto, K. *J. Phys. Chem*. **1986**, 90, 1760.
[66] Will, S.; Lex, J.; Vogel, E.; Adamian, V. A.; van Caemelbecke, E.; Kadish, K. M. *Inorg. Chem*. **1996**, 5577.
[67] Safo, M. K.; Walker, F. A.; Raitsimring, A. M.; Walters, W. P.; Dolata, D. P.; Debrunner, P. G.; Scheidt, W. R. *J. Am. Chem. Soc*. **1994**, 116, 7760.
[68] Mondal, J. U.; Scheidt, W. R. *Unpublished results*.
[69] Minkin, V. L.; Glukhovtsev, M. N.; Simkin, B. Y.; Aromaticity and Antiaromaticity; John Wiley & Sons, New York, 1994.
[70] Telser, J. *Struct. Bonding*, **1998**, 91, 31.
[71] Seth, J.; Palaniappan, V.; Bocian, D. *Inorg. Chem*. **1995**, 34, 2201.
[72] Renner, M. W.; Barkigia, K. M.; Melamed, D.; Smith, K. M.; Fajer, J. *J. Inorg. Chem*. **1996**, 35, 5120.
[73] Ghosh, A.; Wondimagegn, T.; Gonzalez, E.; Halvorsen, I. *J. Inorg. Biochem*. **2000**, 78, 79.
[74] Collins, T. J.; Nichols, E. S.; Uffelman, E. S. *J. Am. Chem. Soc*. **1991**, 113, 4708.
[75] Ghosh, A.; Wondimagegn, T.; Parusel, A. B. J. *J. Am. Chem. Soc.* **2000**, 122, 5100.
[76] Will, S.; Lex, J.; Vogel, E.; Schmickler, H.; Gisselbrecht, J.-P.; Haubtmann, C.; Bernard, M.; Gross, M. *Angew. Chem. Int. Ed. Engl*. **1997**, 36, 357.
[77] Wasbotten, I. H.; Wondimagegn, T.; Ghosh, A. *J. Am. Chem. Soc*. **2002**, 124, 8104.
[78] Wondimagegn, T.; Ghosh, A. *J. Phys. Chem. B*. **2000**, 104, 10858.
[79] Ghosh, A.; Halvorsen, I.; Nilsen, H. J.; Steene, E.; Wondimagegn, T.; Lie, E.; van Caemelbecke, E.; Guo, N.; Ou, Z.; Kadish, K. M. *J. Phys. Chem. B,* **2001**, 105, 8120
[80] Golubkov, G.; Bendix, J.; Gray, H. B.; Mahammed, A.; Goldberg, I.; DiBilio, A. J.; Gross, Z. *Angew. Chem. Int. Ed. Engl*. **2001**, *40*, 2132.
[81] Terner, J.; Gold, A.; Mandon, D.; Trautwein, A. X. *J. Porphyrins Phthalocyanines* **2000**, *5*, 357.
[82] Perdew, J. P.; Chevary, S. H.; Vosko, K. A.; Jackson, M. R.; Singh, D. J.; Fiolhais, C. *Phys. Rev. B*. **1992**, 46, 6671.

[83] Baerends, E. J.; Autschbach, J.A..; Bérces, A..; Bo, C.; Boerrigter, P. M.; Cavallo, L.; Chong, D.P.; Deng, L.; Dickson, R. M.; Ellis, D. E.; Fan, L.; Fischer, T. H.; Fonseca Guerra, C.; van Gisbergen, S. J. A.; Groeneveld, J. A.; Gritsenko, O. V.; Grüning, M.; Harris, F. E.; van den Hoek, P.; Jacobsen, H.; van Kessel, G.; Kootstra, F.; van Lenthe, E.; Osinga, V. P.; Patchkovskii, S.; Philipsen, P. H. T.; Post, D.; Pye, C. C.; Ravenek, W.; Ros, P.; Schipper, P. R. T.; Schreckenbach, G.; Snijders, J. G.; Sola, M. ; Swart, M.; Swerhone, D.; te Velde, G.; Vernooijs, P.; Versluis, L.; Visser, O.; van Wezenbeek, E.; Wiesenekker, G.; Wolff, S. K.; Woo, T. K.; Ziegler, T. *ADF2002.01*, SCM, Theoretical Chemistry, Vrije Universiteit, Amsterdam, The Netherlands, http://www.scm.com.
[84] Flyttet til nr. 12
[85] te Velde, G.; Bickelhaupt, F.M.; van Gisbergen, S. J. A.; Fonseca Guerra, C.; Baerends, E. J.; Snijders, J.G.; Ziegler, T. *J. Comput. Chem*. **2001**, 22, 931.
[86] Fonseca Guerra, C.; Snijders, J.G.; te Velde, G.; Baerends, E. J. *Theor. Chem. Acc*. **1998**, 99, 391.
[87] Ghosh, A.; Gassman, P. G.; Almlöf, J. *J. Am. Chem. Soc*. **1994**, 116, 1932
[88] Ghosh, A.; Fitzgerald, J.; Gassman, P. G.; Almlöf, J. *Inorg. Chem.* **1994**, *33*, 6057.
[89] Tangen, E.; Ghosh, A. *J. Am. Chem. Soc*. **2002**, 124, 8117.
[90] Cai, S; Walker, F. A.; Licoccia, S. *Inorg Chem*, **2000**, 39, 3466.
[91] Simkhovich, L.; Goldberg, I.; Gross, Z. *Inorg. Chem*. **2002**, 41, 5433.
[92] Simkhovich, L.; Galili, N.; Saltsmann, I.; Goldberg, I.; Gross, Z. *Inorg. Chem*. **2000**, *39*, 2704.
[93] Zakharieva, O.; Schünemann, V.; Gerdan, M.; Licoccia, S.; Cai, S.; Walker, F. A.; Trautwein, A. X. *J. Am. Chem. Soc.* **2002**, 124, 6636.
[94] Ramdhanie, B.; Zakharov, L. N.; Rheingold, A. L.; Goldberg, D. P. *Inorg. Chem*. **2002**, 41, 4105.
[95] Mandimutsira, B. S.; Ramdhanie, B.; Todd, R. C.; Wang, H.; Zareba, A. A.; Czernuszewicz, R. S.; Goldberg, D. P. *J. Am. Chem. Soc*. **2002**, 124, 15170.
[96] Vogel, E.; Will, S.; Tilling, A. S.; Neumann, L.; Lex, J.; Bill, E.; Trautwein, A. X.; Wieghardt, K. *Angew. Chem. Int. Ed. Engl*. 1994, 33, 731.
[97] Yatsunyk, L.; Walker, F. A. *Inorg. Chim. Acta*. **2002**, 339C, 171.
[98] Steene, E.; Wondimagegn, T.; Ghosh, A. *J. Inorg. Biochem.* **2002**, 88,113.

8 APPENDIX: OPTIMIZED CARTESIAN COORDINATES

A) $(CZ)P^{V}CL_2[C_{2v}]$

C	-2.447355	0.000000	3.338286
C	-1.149534	0.000000	2.730985
H	-2.594618	0.000000	4.411603
N	-1.321503	0.000000	1.351161
N	0.000000	0.000000	3.391818
C	-3.383145	0.000000	2.341726
N	1.190333	0.000000	-1.189057
C	2.562113	0.000000	-1.198515
H	4.463775	0.000000	2.421486
H	-4.463775	0.000000	2.421486
H	2.594618	0.000000	4.411603
C	1.814892	0.000000	-3.357276
C	-2.705040	0.000000	1.078845
H	3.990560	0.000000	-2.906091
C	-2.958665	0.000000	-2.574614
C	-2.562113	0.000000	-1.198515
H	1.758791	0.000000	-4.439481
N	-1.190333	0.000000	-1.189057
C	2.705040	0.000000	1.078845
C	-1.814892	0.000000	-3.357276
N	-3.312315	0.000000	-0.097875
H	-3.990560	0.000000	-2.906091
H	-1.758791	0.000000	-4.439481
Cl	0.000000	-2.218258	0.148590
C	-0.703375	0.000000	-2.472235
N	3.312315	0.000000	-0.097875
C	0.703375	0.000000	-2.472235
P	0.000000	0.000000	0.142789
C	2.447355	0.000000	3.338286
C	1.149534	0.000000	2.730985
C	2.958665	0.000000	-2.574614
N	1.321503	0.000000	1.351161
Cl	0.000000	2.218258	0.148590
C	3.383145	0.000000	2.341726

B) $(CZ)P^{V}F_2$ [C_{2v}]

C	-2.447895	0.000000	3.322624
C	-1.150199	0.000000	2.712907
H	-2.594884	0.000000	4.396501
N	-1.319610	0.000000	1.331541
N	0.000000	0.000000	3.372890
C	-3.383359	0.000000	2.325682
N	1.189422	0.000000	-1.205543
C	2.560873	0.000000	-1.216391
H	4.464506	0.000000	2.405188
H	-4.464506	0.000000	2.405188
H	2.594884	0.000000	4.396501
C	1.816979	0.000000	-3.376154
C	-2.702505	0.000000	1.062657
H	3.992561	0.000000	-2.925111
C	-2.960378	0.000000	-2.593199
C	-2.560873	0.000000	-1.216391
H	1.762784	0.000000	-4.458925
N	-1.189422	0.000000	-1.205543
C	2.702505	0.000000	1.062657
C	-1.816979	0.000000	-3.376154
N	-3.310716	0.000000	-0.115335
H	-3.992561	0.000000	-2.925111
H	-1.762784	0.000000	-4.458925
F	0.000000	-1.666156	0.136148
C	-0.704230	0.000000	-2.490847
N	3.310716	0.000000	-0.115335
C	0.704230	0.000000	-2.490847
P	0.000000	0.000000	0.124433
C	2.447895	0.000000	3.322624
C	1.150199	0.000000	2.712907
C	2.960378	0.000000	-2.593199
N	1.319610	0.000000	1.331541
F	0.000000	1.666156	0.136148
C	3.383359	0.000000	2.325682

C) (Cz)Cu^{III} [C_{2v}]

Cu	0.000000	0.000000	-0.140546
H	0.000000	2.616489	-4.430112
H	0.000000	-1.799580	4.466953
H	0.000000	4.486345	-2.449888
H	0.000000	-4.009652	2.920083
H	0.000000	-2.616489	-4.430112
H	0.000000	1.799580	4.466953
H	0.000000	4.009652	2.920083
H	0.000000	-4.486345	-2.449888
N	0.000000	1.359184	-1.371901
N	0.000000	-1.206319	1.227151
N	0.000000	-1.359184	-1.371901
N	0.000000	1.206319	1.227151
C	0.000000	2.466532	-3.356278
C	0.000000	-1.838272	3.383563
C	0.000000	3.405671	-2.360830
C	0.000000	-2.976172	2.591944
C	0.000000	1.162783	-2.737963
C	0.000000	-0.707883	2.510259
C	0.000000	2.720564	-1.089223
C	0.000000	-2.568327	1.210820
N	0.000000	0.000000	-3.389054
N	0.000000	3.318014	0.101137
N	0.000000	-3.318014	0.101137
C	0.000000	-1.162783	-2.737963
C	0.000000	0.707883	2.510259
C	0.000000	2.568327	1.210820
C	0.000000	-2.720564	-1.089223
C	0.000000	-2.466532	-3.356278
C	0.000000	1.838272	3.383563
C	0.000000	2.976172	2.591944
C	0.000000	-3.405671	-2.360830

D) (Cz)Fe^{IV}Cl [C_S]

C	3.283941	0.219748	2.458988
C	2.666252	0.122825	1.163609
H	4.354543	0.296007	2.610257
N	1.291001	0.038659	1.342504
N	3.311229	0.143878	0.000000
C	2.285376	0.206026	3.398418
N	-1.286219	-0.025360	-1.193283
C	-1.280137	0.106790	-2.560346
H	2.372375	0.281762	-4.475992
H	2.372375	0.281762	4.475992
H	4.354543	0.296007	-2.610257
C	-3.435637	0.292405	-1.827488
C	1.025154	0.101434	2.707987
H	-2.970086	0.417879	-3.992938
C	-2.648799	0.284409	2.966240
C	-1.280137	0.106790	2.560346
H	-4.508501	0.439984	-1.780346
N	-1.286219	-0.025360	1.193283
C	1.025154	0.101434	-2.707987
C	-3.435637	0.292405	1.827488
N	-0.173306	0.135354	3.300295
H	-2.970086	0.417879	3.992938
H	-4.508501	0.439984	1.780346
Cl	0.124794	-2.566301	0.000000
C	-2.564675	0.104215	0.708442
N	-0.173306	0.135354	-3.300295
C	-2.564675	0.104215	-0.708442
Fe	0.077086	-0.425087	0.000000
C	3.283941	0.219748	-2.458988
C	2.666252	0.122825	-1.163609
C	-2.648799	0.284409	-2.966240
N	1.291001	0.038659	-1.342504
C	2.285376	0.206026	-3.398418

E) (CZ)MN^{IV}CL [C_S]

C	3.277574	0.254937	2.465632
C	2.665451	0.125075	1.170478
H	4.345412	0.361458	2.615907
N	1.288288	0.027507	1.361514
N	3.297858	0.153587	0.000000
C	2.280805	0.248175	3.407152
N	-1.307463	-0.063892	-1.205910
C	-1.295498	0.109866	-2.569670
H	2.371705	0.352633	-4.481891
H	2.371705	0.352633	4.481891
H	4.345412	0.361458	-2.615907
C	-3.442622	0.351446	-1.822966
C	1.018059	0.114741	2.726300
H	-2.977366	0.520282	-3.986357
C	-2.659011	0.343564	2.965348
C	-1.295498	0.109866	2.569670
H	-4.508902	0.538756	-1.768589
N	-1.307463	-0.063892	1.205910
C	1.018059	0.114741	-2.726300
C	-3.442622	0.351446	1.822966
N	-0.184747	0.154532	3.305787
H	-2.977366	0.520282	3.986357
H	-4.508902	0.538756	1.768589
Cl	0.186893	-2.645706	0.000000
C	-2.576732	0.107267	0.710267
N	-0.184747	0.154532	-3.305787
C	-2.576732	0.107267	-0.710267
Mn	0.088771	-0.476457	0.000000
C	3.277574	0.254937	-2.465632
C	2.665451	0.125075	-1.170478
C	-2.659011	0.343564	-2.965348
N	1.288288	0.027507	-1.361514
C	2.280805	0.248175	-3.407152

F) (COR)$P^{V}F_2$ [C_{2v}]

C	-2.508057	0.000000	3.364482
C	-1.216882	0.000000	2.759447
H	-2.675057	0.000000	4.436003
N	-1.364690	0.000000	1.377575
C	0.000000	0.000000	3.418488
H	0.000000	0.000000	4.504979
C	-3.436959	0.000000	2.359861
N	1.204783	0.000000	-1.231554
C	2.579426	0.000000	-1.298315
H	4.518303	0.000000	2.445134
H	-4.518303	0.000000	2.445134
H	2.675057	0.000000	4.436003
C	1.774779	0.000000	-3.427712
C	-2.743399	0.000000	1.113239
H	3.961534	0.000000	-3.045505
C	-2.941321	0.000000	-2.676756
C	-2.579426	0.000000	-1.298315
H	1.683764	0.000000	-4.508055
N	-1.204783	0.000000	-1.231554
C	2.743399	0.000000	1.113239
C	-1.774779	0.000000	-3.427712
C	-3.339193	0.000000	-0.137433
H	-4.423818	0.000000	-0.196105
H	-3.961534	0.000000	-3.045505
H	-1.683764	0.000000	-4.508055
F	0.000000	-1.655830	0.158978
C	-0.700630	0.000000	-2.510170
C	3.339193	0.000000	-0.137433
H	4.423818	0.000000	-0.196105
C	0.700630	0.000000	-2.510170
P	0.000000	0.000000	0.137668
C	2.508057	0.000000	3.364482
C	1.216882	0.000000	2.759447
C	2.941321	0.000000	-2.676756
N	1.364690	0.000000	1.377575
F	0.000000	1.655830	0.158978
C	3.436959	0.000000	2.359861

G) (COR)CU^{III} [C_{2v}]

Cu	0.00000	0.00000	-0.15600
H	0.00000	2.69700	-4.47200
H	0.00000	-1.72300	4.51800
H	0.00000	4.54400	-2.49500
H	0.00000	-3.98100	3.03900
H	0.00000	-2.69700	-4.47200
H	0.00000	1.72300	4.51800
H	0.00000	3.98100	3.03900
H	0.00000	-4.54400	-2.49500
H	0.00000	0.00000	-4.52200
H	0.00000	4.43300	0.19100
H	0.00000	-4.43300	0.19100
N	0.00000	1.40600	-1.41700
N	0.00000	-1.22100	1.25500
N	0.00000	-1.40600	-1.41700
N	0.00000	1.22100	1.25500
C	0.00000	2.52800	-3.40000
C	0.00000	-1.79700	3.43600
C	0.00000	3.46300	-2.39800
C	0.00000	-2.95900	2.67500
C	0.00000	1.23100	-2.78600
C	0.00000	-0.70500	2.53100
C	0.00000	2.76800	-1.14300
C	0.00000	-2.58900	1.29200
C	0.00000	0.00000	-3.43400
C	0.00000	3.34800	0.12200
C	0.00000	-3.34800	0.12200
C	0.00000	-1.23100	-2.78600
C	0.00000	0.70500	2.53100
C	0.00000	2.58900	1.29200
C	0.00000	-2.76800	-1.14300
C	0.00000	-2.52800	-3.40000
C	0.00000	1.79700	3.43600
C	0.00000	2.95900	2.67500
C	0.00000	-3.46300	-2.39800

H) (COR)FE^{IV}CL [C_S]

Fe	0.132989	0.404454	0.000000
H	4.449264	-0.167709	-2.707984
H	-4.535254	-0.237492	1.716060
H	2.468933	-0.136944	-4.545694
H	-3.076301	-0.183238	3.976927
H	4.449264	-0.167709	2.707984
H	-4.535254	-0.237492	-1.716060
H	-3.076301	-0.183238	-3.976927
H	2.468933	-0.136944	4.545694
H	4.485708	-0.116589	0.000000
H	-0.220324	-0.069805	-4.416413
H	-0.220324	-0.069805	4.416413
N	1.386647	-0.010773	-1.396588
N	-1.268420	0.006998	1.208913
N	1.386647	-0.010773	1.396588
N	-1.268420	0.006998	-1.208913
C	3.379968	-0.117070	-2.532189
C	-3.457172	-0.152290	1.795521
C	2.373509	-0.096482	-3.465591
C	-2.705876	-0.126795	2.958907
C	2.761912	-0.061501	-1.240628
C	-2.539912	-0.067656	0.708580
C	1.127457	-0.030542	-2.758195
C	-1.325157	-0.033244	2.584657
C	3.397463	-0.074831	0.000000
C	-0.153766	-0.034307	-3.330675
C	-0.153766	-0.034307	3.330675
C	2.761912	-0.061501	1.240628
C	-2.539912	-0.067656	-0.708580
C	-1.325157	-0.033244	-2.584657
C	1.127457	-0.030542	2.758195
C	3.379968	-0.117070	2.532189
C	-3.457172	-0.152290	-1.795521
C	-2.705876	-0.126795	-2.958907
C	2.373509	-0.096482	3.465591
Cl	0.179114	2.574862	0.000000

I) (COR)MN^{IV}CL [C_S]

Mn	0.404939	-0.168444	0.000000
H	-0.300697	-4.461853	-2.716353
H	-0.308875	4.526769	1.714759
H	-0.242465	-2.490451	-4.556490
H	-0.238671	3.071412	3.974557
H	-0.300697	-4.461853	2.716353
H	-0.308875	4.526769	-1.714759
H	-0.238671	3.071412	-3.974557
H	-0.242465	-2.490451	4.556490
H	-0.220954	-4.497198	0.000000
H	-0.111662	0.219894	-4.423175
H	-0.111662	0.219894	4.423175
N	-0.051593	-1.407924	-1.419461
N	0.004053	1.270269	1.216475
N	-0.051593	-1.407924	1.419461
N	0.004053	1.270269	-1.216475
C	-0.215964	-3.394436	-2.541405
C	-0.196273	3.451896	1.794384
C	-0.183164	-2.390404	-3.477911
C	-0.157275	2.701247	2.958359
C	-0.129524	-2.781151	-1.248549
C	-0.089957	2.537811	0.708902
C	-0.079108	-1.141195	-2.779022
C	-0.040391	1.321519	2.590121
C	-0.153129	-3.410324	0.000000
C	-0.062721	0.146525	-3.338556
C	-0.062721	0.146525	3.338556
C	-0.129524	-2.781151	1.248549
C	-0.089957	2.537811	-0.708902
C	-0.040391	1.321519	-2.590121
C	-0.079108	-1.141195	2.779022
C	-0.215964	-3.394436	2.541405
C	-0.196273	3.451896	-1.794384
C	-0.157275	2.701247	-2.958359
C	-0.183164	-2.390404	3.477911
Cl	2.603787	-0.238147	0.000000

J) (COR)Co^{IV}CL [C_S]

Co	0.131046	0.300537	0.000000
H	4.448905	-0.165176	-2.704286
H	-4.536740	-0.211974	1.717528
H	2.466421	-0.108839	-4.539523
H	-3.067382	-0.174468	3.970498
H	4.448905	-0.165176	2.704286
H	-4.536740	-0.211974	-1.717528
H	-3.067382	-0.174468	-3.970498
H	2.466421	-0.108839	4.539523
H	4.491312	-0.098625	0.000000
H	-0.211471	-0.035885	-4.404653
H	-0.211471	-0.035885	4.404653
N	1.393453	0.011395	-1.385555
N	-1.264445	0.043804	1.205991
N	1.393453	0.011395	1.385555
N	-1.264445	0.043804	-1.205991
C	3.380520	-0.097915	-2.531076
C	-3.459896	-0.122757	1.795764
C	2.376901	-0.062731	-3.459840
C	-2.705041	-0.112191	2.950452
C	2.761955	-0.040342	-1.236193
C	-2.544341	-0.025330	0.702434
C	1.132006	0.009016	-2.747759
C	-1.317756	-0.005311	2.569850
C	3.403271	-0.055207	0.000000
C	-0.144441	0.002516	-3.318811
C	-0.144441	0.002516	3.318811
C	2.761955	-0.040342	1.236193
C	-2.544341	-0.025330	-0.702434
C	-1.317756	-0.005311	-2.569850
C	1.132006	0.009016	2.747759
C	3.380520	-0.097915	2.531076
C	-3.459896	-0.122757	-1.795764
C	-2.705041	-0.112191	-2.950452
C	2.376901	-0.062731	3.459840
Cl	0.157825	2.508044	0.000000

K) (COR)FE^{IV}PH [C_S], CONFIGURATION 1

Fe	-0.180577	0.310344	0.000000
H	3.151059	3.095266	2.706021
H	-2.897527	-3.540769	-1.706100
H	1.781753	1.667772	4.543647
H	-1.909171	-2.461487	-3.967583
H	3.151059	3.095266	-2.706021
H	-2.897527	-3.540769	1.706100
H	-1.909171	-2.461487	3.967583
H	1.781753	1.667772	-4.543647
H	3.142367	3.168569	0.000000
H	-0.083099	-0.261773	4.419818
H	-0.083099	-0.261773	-4.419818
N	0.926334	0.989527	1.391066
N	-0.931762	-0.908794	-1.216065
N	0.926334	0.989527	-1.391066
N	-0.931762	-0.908794	1.216065
C	2.377785	2.354254	2.530178
C	-2.247194	-2.676386	-1.786068
C	1.677823	1.633010	3.464183
C	-1.731998	-2.122473	-2.952142
C	1.910753	1.951178	1.235691
C	-1.734621	-1.913987	-0.704580
C	0.772446	0.772251	2.762273
C	-0.894198	-1.021221	-2.582704
C	2.361965	2.409893	0.000000
C	-0.086698	-0.167022	3.336158
C	-0.086698	-0.167022	-3.336158
C	1.910753	1.951178	-1.235691
C	-1.734621	-1.913987	0.704580
C	-0.894198	-1.021221	2.582704
C	0.772446	0.772251	-2.762273
C	2.377785	2.354254	-2.530178
C	-2.247194	-2.676386	1.786068
C	-1.731998	-2.122473	2.952142
C	1.677823	1.633010	-3.464183
C	-1.986400	2.257013	1.217687
C	-1.986400	2.257013	-1.217687
C	-2.923854	3.293413	-1.211657
C	-2.923854	3.293413	1.211657
C	-3.392646	3.813041	0.000000
C	-1.522390	1.743784	0.000000
H	-1.633525	1.860917	-2.169173
H	-1.633525	1.860917	2.169173
H	-3.288039	3.690240	-2.159656
H	-3.288039	3.690240	2.159656
H	-4.121253	4.623621	0.000000

L) (COR)Fe^{IV}PH [C_S], CONFIGURATION 2

Fe	-0.204755	0.357559	0.000000
H	3.318988	2.931383	2.694636
H	-2.817445	-3.573662	-1.695438
H	1.913855	1.540683	4.535347
H	-1.822114	-2.502878	-3.958871
H	3.318988	2.931383	-2.694636
H	-2.817445	-3.573662	1.695438
H	-1.822114	-2.502878	3.958871
H	1.913855	1.540683	-4.535347
H	3.263397	3.055378	0.000000
H	-0.023174	-0.300418	4.416669
H	-0.023174	-0.300418	-4.416669
N	0.926575	1.007990	1.391489
N	-0.950047	-0.869053	-1.217466
N	0.926575	1.007990	-1.391489
N	-0.950047	-0.869053	1.217466
C	2.487964	2.254233	2.524825
C	-2.202714	-2.683849	-1.780245
C	1.772295	1.549901	3.459584
C	-1.683295	-2.134995	-2.947006
C	1.963615	1.911409	1.235758
C	-1.731194	-1.888822	-0.705024
C	0.801726	0.760617	2.763037
C	-0.883697	-1.006281	-2.582376
C	2.429910	2.354810	0.000000
C	-0.056144	-0.175273	3.336396
C	-0.056144	-0.175273	-3.336396
C	1.963615	1.911409	-1.235758
C	-1.731194	-1.888822	0.705024
C	-0.883697	-1.006281	2.582376
C	0.801726	0.760617	-2.763037
C	2.487964	2.254233	-2.524825
C	-2.202714	-2.683849	1.780245
C	-1.683295	-2.134995	2.947006
C	1.772295	1.549901	-3.459584
C	-2.943813	1.409926	0.000000
C	-1.202048	3.102953	0.000000
C	-3.913643	2.417755	0.000000
C	-2.182193	4.101784	0.000000
C	-3.537280	3.763348	0.000000
C	-1.589834	1.759557	0.000000
H	-0.149993	3.389562	0.000000
H	-3.258318	0.366427	0.000000
H	-1.876351	5.148791	0.000000
H	-4.968789	2.140966	0.000000
H	-4.298006	4.545167	0.000000

M) (COR)MN^{IV}PH [C_S], CONFIGURATION 1

Mn	-0.226655	0.275285	-0.000000
H	2.870359	3.280656	2.715601
H	-2.733267	-3.759100	-1.713528
H	1.621118	1.761909	4.560492
H	-1.806388	-2.634922	-3.972501
H	2.870359	3.280656	-2.715601
H	-2.733267	-3.759100	1.713528
H	-1.806388	-2.634922	3.972501
H	1.621118	1.761909	-4.560492
H	2.855208	3.338481	-0.000000
H	-0.118331	-0.326007	4.433502
H	-0.118331	-0.326007	-4.433502
N	0.870328	0.963092	1.420225
N	-0.941467	-1.014112	-1.226267
N	0.870328	0.963092	-1.420225
N	-0.941467	-1.014112	1.226267
C	2.173900	2.467978	2.540093
C	-2.138458	-2.854481	-1.791984
C	1.533903	1.696344	3.480321
C	-1.655256	-2.275658	-2.959824
C	1.759007	2.012716	1.245785
C	-1.676737	-2.059797	-0.708508
C	0.709993	0.748981	2.786461
C	-0.884545	-1.123402	-2.595125
C	2.159230	2.501725	-0.000000
C	-0.112846	-0.233667	3.349164
C	-0.112846	-0.233667	-3.349164
C	1.759007	2.012716	-1.245785
C	-1.676737	-2.059797	0.708508
C	-0.884545	-1.123402	2.595125
C	0.709993	0.748981	-2.786461
C	2.173900	2.467978	-2.540093
C	-2.138458	-2.854481	1.791984
C	-1.655256	-2.275658	2.959824
C	1.533903	1.696344	-3.480321
C	-1.918613	2.355269	1.217825
C	-1.918613	2.355269	-1.217825
C	-2.613891	3.571420	-1.222596
C	-2.613891	3.571420	1.222596
C	-2.947695	4.185380	-0.000000
C	-1.539928	1.773910	-0.000000
H	-1.657997	1.883862	-2.166660
H	-1.657997	1.883862	2.166660
H	-2.902336	4.027326	-2.170740
H	-2.902336	4.027326	2.170740
H	-3.488776	5.132286	-0.000000

N) (COR)MN^{IV}PH [C_S], CONFIGURATION 2

Mn	-0.170263	0.343839	-0.000000
H	3.259304	3.011508	2.712593
H	-2.901445	-3.535438	-1.718885
H	1.883170	1.606263	4.555458
H	-1.902534	-2.464501	-3.975805
H	3.259304	3.011508	-2.712593
H	-2.901445	-3.535438	1.718885
H	-1.902534	-2.464501	3.975805
H	1.883170	1.606263	-4.555458
H	3.212658	3.111733	-0.000000
H	-0.054476	-0.289244	4.429330
H	-0.054476	-0.289244	-4.429330
N	0.957666	0.990396	1.419257
N	-0.931368	-0.918856	-1.224407
N	0.957666	0.990396	-1.419257
N	-0.931368	-0.918856	1.224407
C	2.457395	2.301723	2.539358
C	-2.248210	-2.672921	-1.794965
C	1.754703	1.586369	3.477805
C	-1.729459	-2.120382	-2.961329
C	1.962709	1.928093	1.246246
C	-1.732812	-1.915137	-0.709388
C	0.812181	0.754847	2.786239
C	-0.889012	-1.020957	-2.593877
C	2.410012	2.376302	-0.000000
C	-0.060178	-0.181898	3.346378
C	-0.060178	-0.181898	-3.346378
C	1.962709	1.928093	-1.246246
C	-1.732812	-1.915137	0.709388
C	-0.889012	-1.020957	2.593877
C	0.812181	0.754847	-2.786239
C	2.457395	2.301723	-2.539358
C	-2.248210	-2.672921	1.794965
C	-1.729459	-2.120382	2.961329
C	1.754703	1.586369	-3.477805
C	-2.927152	1.406892	-0.000000
C	-1.187592	3.098782	-0.000000
C	-3.897531	2.413697	-0.000000
C	-2.165386	4.098508	-0.000000
C	-3.520422	3.759079	-0.000000
C	-1.571657	1.754076	-0.000000
H	-0.135381	3.385858	-0.000000
H	-3.241512	0.363391	-0.000000
H	-1.859463	5.145448	-0.000000
H	-4.952819	2.138093	-0.000000
H	-4.280265	4.541230	-0.000000

O) (COR)Co^{IV}PH [C_S], CONFIGURATION 1

Co	-0.126199	0.269336	0.000000
H	3.165135	3.090782	2.706812
H	-2.926304	-3.511536	-1.703823
H	1.794455	1.661757	4.541349
H	-1.915243	-2.445611	-3.955204
H	3.165135	3.090782	-2.706812
H	-2.926304	-3.511536	1.703823
H	-1.915243	-2.445611	3.955204
H	1.794455	1.661757	-4.541349
H	3.135170	3.187901	0.000000
H	-0.090230	-0.242006	4.406068
H	-0.090230	-0.242006	-4.406068
N	0.916527	1.018119	1.383829
N	-0.959144	-0.866454	-1.212334
N	0.916527	1.018119	-1.383829
N	-0.959144	-0.866454	1.212334
C	2.380659	2.361594	2.533422
C	-2.278519	-2.646912	-1.784178
C	1.684246	1.642737	3.462506
C	-1.754422	-2.101971	-2.939117
C	1.896383	1.970198	1.232563
C	-1.773269	-1.873969	-0.697416
C	0.762715	0.793825	2.752307
C	-0.914256	-0.985928	-2.562535
C	2.350035	2.434232	0.000000
C	-0.096383	-0.138743	3.322766
C	-0.096383	-0.138743	-3.322766
C	1.896383	1.970198	-1.232563
C	-1.773269	-1.873969	0.697416
C	-0.914256	-0.985928	2.562535
C	0.762715	0.793825	-2.752307
C	2.380659	2.361594	-2.533422
C	-2.278519	-2.646912	1.784178
C	-1.754422	-2.101971	2.939117
C	1.684246	1.642737	-3.462506
C	-1.969457	2.186676	1.211385
C	-1.969457	2.186676	-1.211385
C	-2.907553	3.228519	-1.203751
C	-2.907553	3.228519	1.203751
C	-3.381206	3.752745	0.000000
C	-1.500348	1.676969	0.000000
H	-1.617317	1.803835	-2.167462
H	-1.617317	1.803835	2.167462
H	-3.259016	3.627278	-2.156219
H	-3.259016	3.627278	2.156219
H	-4.103544	4.569802	0.000000

P) (COR)Co^{IV}PH [C_S], CONFIGURATION 2

Co	-0.128131	0.285113	0.000000
H	3.240618	3.021529	2.705349
H	-2.899165	-3.516776	-1.704641
H	1.823140	1.641426	4.544434
H	-1.911921	-2.430347	-3.959431
H	3.240618	3.021529	-2.705349
H	-2.899165	-3.516776	1.704641
H	-1.911921	-2.430347	3.959431
H	1.823140	1.641426	-4.544434
H	3.204750	3.122261	0.000000
H	-0.103551	-0.220563	4.411249
H	-0.103551	-0.220563	-4.411249
N	0.923349	1.021172	1.386959
N	-0.952375	-0.858512	-1.212838
N	0.923349	1.021172	-1.386959
N	-0.952375	-0.858512	1.212838
C	2.428435	2.321837	2.534907
C	-2.262112	-2.643208	-1.786674
C	1.709551	1.625400	3.465254
C	-1.750241	-2.088589	-2.941791
C	1.931897	1.942315	1.234856
C	-1.754070	-1.871318	-0.699109
C	0.764822	0.801228	2.757490
C	-0.916564	-0.968803	-2.565872
C	2.395042	2.394576	0.000000
C	-0.103224	-0.121981	3.327545
C	-0.103224	-0.121981	-3.327545
C	1.931897	1.942315	-1.234856
C	-1.754070	-1.871318	0.699109
C	-0.916564	-0.968803	2.565872
C	0.764822	0.801228	-2.757490
C	2.428435	2.321837	-2.534907
C	-2.262112	-2.643208	1.786674
C	-1.750241	-2.088589	2.941791
C	1.709551	1.625400	-3.465254
C	-2.867820	1.330896	0.000000
C	-1.123231	3.011290	0.000000
C	-3.833933	2.343598	0.000000
C	-2.098394	4.016487	0.000000
C	-3.454769	3.688124	0.000000
C	-1.513045	1.670800	0.000000
H	-0.072560	3.298845	0.000000
H	-3.195245	0.292182	0.000000
H	-1.783538	5.061010	0.000000
H	-4.889780	2.068648	0.000000
H	-4.211570	4.473462	0.000000